INTERACTIONS BETWEEN DNA DOUBLE-STRAND BREAK REPAIR PROTEINS AND THE TELOMERASE DNA REPLICATION COMPLEX

THESIS

Presented to the Graduate Council
of Texas State University-San Marcos
in Partial Fulfillment
of the Requirements

for the Degree

Master of SCIENCE

by

Brian M. Wasko, B.S.

San Marcos, Texas
August 2006

ACKNOWLEDGEMENTS

I would like to thank Dr. Lewis for his exceptional guidance and instruction during the past few years. He is an ideal mentor, providing his time and knowledge while retaining endless patience. I am very grateful for the opportunity to have worked under his supervision.

I would also like to thank all of my lab mates throughout the years. There are far too many to mention them all, but each of them was not only a colleague, but a true friend. I must thank Shanna and Jared for providing a foundation for my research, and also for their friendship. Hiranthi and Allison thank you for your companionship, and I wish you the best in your current and future endeavors. To Veera and Sandra, I hope your time in the lab will be as extraordinary as mine was. I would also like to thank my thesis committee, Dr. Rachell Booth and Dr. James Irvin for their input and time.

I must also thank my family. You all have had endless faith in me and provided more love and support than I could ask for. Last, but not least, thank you Jaci. We have shared this tremendous experience of graduate school together, and I look foreword to what the future has in store for us.

TABLE OF CONTENTS

LIST OF TABLES

Page

TABLE

LIST OF FIGURES

Page

FIGURE

CHAPTER I

INTRODUCTION

The genetic instructions required for life are contained within the code of an organism's deoxyribonucleic acid (DNA). DNA exists as highly compacted double helical strands known as chromosomes, located within the cell nucleus of eukaryotes. Due to its many functional groups, chromosomal DNA is subject to chemical alteration by a variety of methods, which can result in lesions on one or both of the DNA strands. Double-strand breaks (DSBs) are currently considered to be the most lethal type of DNA damage in eukaryotes (1). If a DSB is not accurately repaired, the break may result in mutations, abnormal recombination events, "capping" by *de novo* telomere addition, or apoptosis. These consequences of DSBs could lead to cell death, altered metabolism, or cancer development. Causes of DSBs include many endogenous and exogenous mechanisms, including physical agents such as X-rays and chemical agents such as the anti-tumor drug bleomycin and the chemical methyl methanesulfonate (MMS) (2, 3). Agents that cause DSBs commonly elevate the risk for cancer, among other human and animal diseases (4).

Typical research techniques induce DSBs by either treatment with chemical or physical DNA-damaging agents or restriction endonuclease enzymes. The former produces a variety of types of DNA damage and does not allow site-specific breaks. Endonucleases such as *Eco*RI recognize and cleave at specific sequences and can be

manipulated by regulatable promoters, which permit greater control of DSB induction. The DSB ends produced by endonucleases are much more defined compared to those produced by DNA-damaging agents, allowing for differential analysis dependent upon the selected method of DSB induction.

The model organism *Saccharomyces cerevisiae* (budding yeast) is an ideal organism to study for a variety of reasons. *Saccharomyces cerevisiae* was one of the first organisms to have its genome sequenced and was the first eukaryote to be transformed with plasmids. As a eukaryote, its complex internal cell structure is analogous to that of plants and animals, however it maintains short generation times allowing for rapid experimentation. This budding yeast also contains numerous genes that are highly conserved with those of higher eukaryotes (5). In fact, many gene products important in human biology were first discovered by studying their yeast homologs. Many advanced molecular genetic and molecular biology techniques have been developed with *S. cerevisiae*.

In eukaryotes, there are at least two conserved pathways responsible for repair of DSBs, the non-homologous endjoining (NHEJ) pathway and the homologous recombination pathway (Figure 1). Homologous recombination requires that a sequence of exact or near exact homology be utilized as a template for repair of a DSB. The first step of homologous recombination is 5' to 3' end resection of the DNA producing 3' overhangs. This is followed by Rad52 epistasis group mediated recombination (strand exchange). NHEJ involves direct joining of DNA ends irrespective of their sequence and has a greater tendency to be mutagenic than homologous recombination (3). In *S. cerevisiae*, the NHEJ pathway consists of at least four complexes: Yku70/Yku80,

Sir2/Sir3/Sir4, Dnl4/Lif1/Nej1 and Rad50/Mre11/Xrs2. The recombination pathway requires the Rad51/Rad52/Rad54/Rad55/Rad57 and Rad50/Mre11/Xrs2 complexes, as well as several other proteins that are not well elucidated.

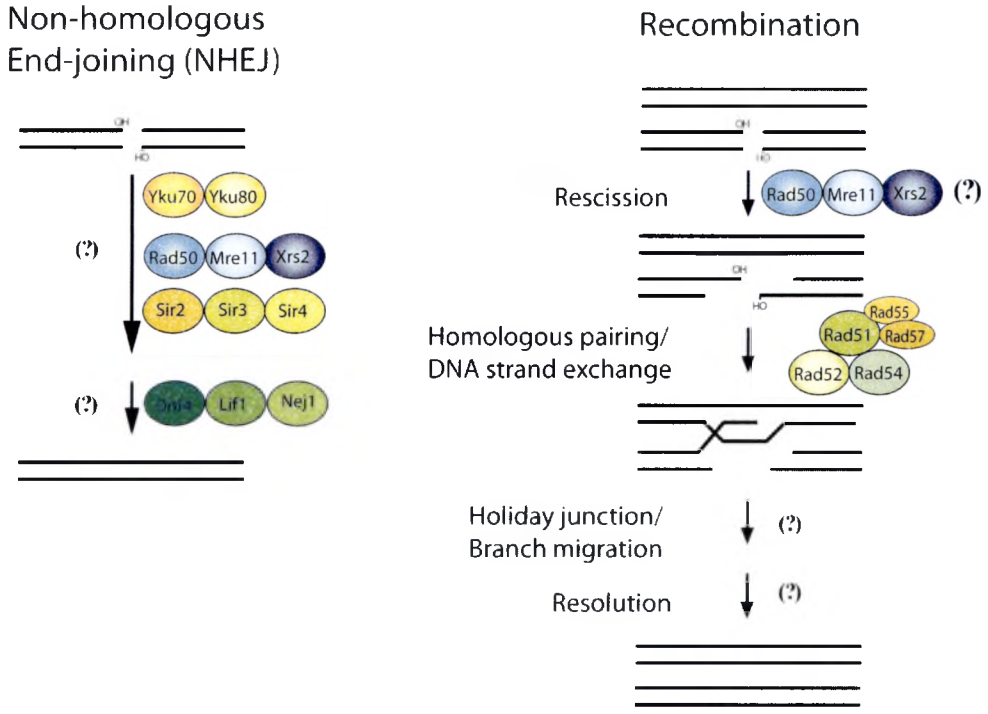

Figure 1. Schematic of the NHEJ and homologous recombination pathways.

Rad50, Mre11, and Xrs2 (RMX) form a protein complex that is unique due to its involvement in both the NHEJ and recombination pathways. Rad50 is a Zn^{2+} and Mg^{2+}-dependent protein that is thought to recruit the RMX complex to DNA ends in the presence of ATP (6). Mre11 is a Mn^{2+}-dependent 3'-to-5' single-stranded DNA (ssDNA) and double-stranded DNA (dsDNA) exonuclease and ssDNA endonuclease utilized in formation of 3' ssDNA overhangs (7). Mre11 also contains several highly conserved phosphodiester motifs and two DNA binding domains (8). Also, Mre11 has a role in maintenance of telomeres (9). Little is known about Xrs2, but it has recently been shown

to act as a specificity factor for the RMX complex (10), and might be involved in RMX repair within NHEJ via an interaction with Lif1 (11). The RMX complex is thought to bind DNA DSBs and hold them in close proximity as in the "headphone" model shown in Figure 2. Evidence supports RMX requiring its nuclease activity for recombinational repair and telomere maintenance, but not for NHEJ (12, 13). Even though the RMX complex contains 3' to 5' exonuclease activity and homologous recombination requires production of a 3' overhang, it may be that the endonuclease activity produces the 3' overhang by an unknown mechanism (14). Deletion of any of the three genes of the RMX complex causes inactivation of the entire protein complex, which leads to reduced levels of NHEJ and recombination, sensitivity to DSBs, and shortened telomeres (15). Nijmegen Breakage Syndrome and Ataxia Telangiectasia-like Disorder are human diseases in which human gene homologs of the RMX complex are mutated. Both of these disorders are characterized by sensitivity to ionizing radiation and a predisposition to cancer formation (16).

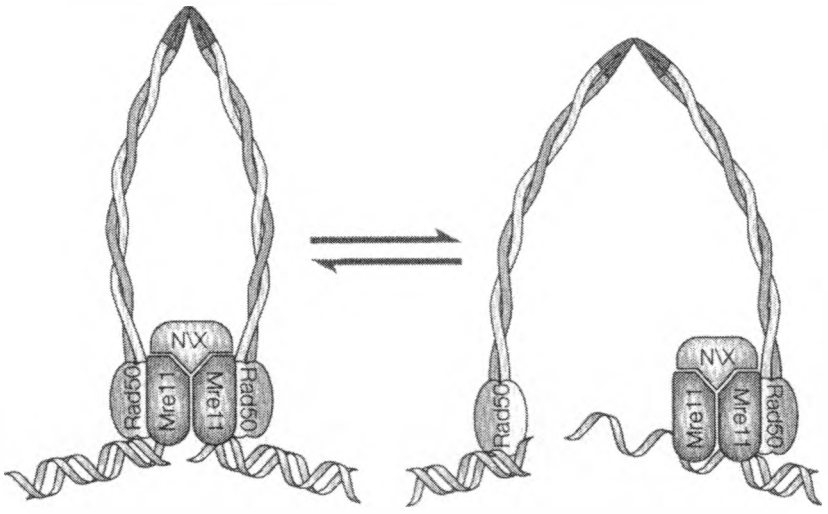

Figure 2. Headphone model of RMX complex binding to broken DNA ends. The DSB ends are held in close proximity by RMX and a 3' overhang is generated by Mre11.

During DNA replication, a short RNA primer is generated for use in DNA synthesis. This RNA primer is later degraded and the RNA nucleotides are replaced with the appropriate DNA nucleotides. As DNA is synthesized in the 5' to 3' direction, at the extreme 5' ends of the chromosome, the degradation of RNA primers poses a problem; there is an absence of a 3' hydroxyl for nucleotide addition, which would result in a progressive shortening of the chromosome. This is known as the "end replication problem" (Figure 3). Cells combat a potential loss of genetic information by maintaining non-coding repeating nucleotide sequences at the ends of linear chromosomes, known as telomeres. These telomeres and telomere-associated proteins provide a cap for the chromosome ends. With at least mammalian telomeres, the 3' single-stranded DNA overhang can loop back and anneal with complementary internal

sequences forming a "t-loop" that may also provide structural protection for the end (17). The telomeres are thought to switch stochastically from capped to uncapped states (18). In the uncapped state, the telomeres appear similar to DSBs, which could cause a DNA damage response, and would then be susceptible to detrimental processes such as fusion with other telomeres or broken DNA ends, nuclease degradation, and illegitimate recombination. The telomeres are vulnerable to the end replication problem and progressively shorten in most human somatic cells. The solution to this progressive shortening of the telomeres lies in an enzyme known as telomerase. Telomerase is a reverse transcriptase that extends the 3' ends of linear chromosomes, allowing for further extension of the complementary strand by conventional replication processes (Figure 4).

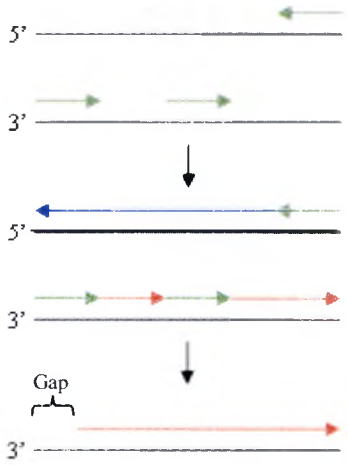

Figure 3. The end replication problem. Short RNA sequences (green) provide a primer for DNA synthesis. Leading strand synthesis (blue) is able to extend to the chromosome end. After primer removal, lagging strand synthesis (red) results in a gap with a loss of nucleotides.

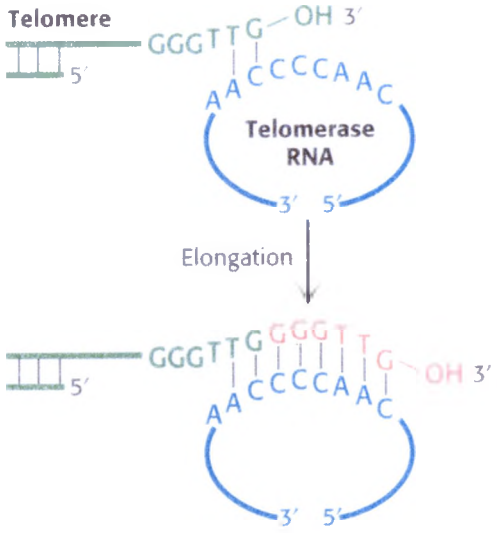

Figure 4. Telomerase polymerization. Telomerase RNA anneals and provides a template for extension of the 3' end by the telomerase polymerase. Telomerase can then translocate and repeat this process.

During normal human somatic cell aging, there is a gradual loss of telomeric DNA length, which is proposed to contribute to mortality in many age-related diseases (19). Human telomerase is expressed in the highly proliferative germ and stem cells but not in normal somatic cells (20). Cells that are deficient in telomerase activity have progressive telomere shortening and eventually undergo cellular senescence (loss of ability to grow) (18). There are mechanisms that allow alternative lengthening of chromosome ends by recombination between telomeres, but telomerase is thought to provide the primary means for telomere stabilization (18).

High telomerase activity is a hallmark of cancer in over 90% of human cancer cells (21). Telomerase allows cancer cells to replicate indefinitely and thus allows for tumor growth and metastasis. Detection of telomerase has potential utility for cancer

diagnosis, prognosis, screening and monitoring. Inhibiting telomerase activity is a potential universal target for cancer treatment, and in fact there is a telomerase inhibitor created by Geron Corporation (Menlo Park, CA) suggested for use against multiple cancers. This drug is currently in phase I/II clinical trials for patients with advanced chronic lymphocytic leukemia and in a phase I clinical trial for patients with solid tumor malignancies (22, 23, 24, 25). There is also a telomerase cancer vaccine in phase I/II clinical trials for patients with prostate cancer aimed at utilizing the immune system to specifically attack cancer cells (26).

Maintenance of telomeres in *S. cerevisiae* involves many different genes, including genes that encode telomerase subunits such as *EST1, EST2, EST3, CDC13,* and *TLC1*, as well as several other genes that are also known to have an impact on chromatin structure, such as *SIR2*, *SIR3, SIR4, YKU70,* and *YKU80* (12). In addition, Ten1 and Stn1 have been found to associate with telomerase by binding with Cdc13, and are proposed to be required for telomere length regulation and DNA damage protection (27).

In vitro, telomerase function requires *TLC1,* which is the 1301 nucleotide (nt) RNA template component, and *EST2*, which is the catalytic polymerase subunit. *In vivo*, telomerase function requires at least *TLC1*, *EST1*, *EST2*, *EST3*, and *CDC13*. *TLC1* RNA not only provides a template for elongation, but also contains protein interacting regions and provides a scaffold for the assembly of the telomerase proteins (28) (Figure 5). The template region of *TLC1* RNA contains 17 nt composed of CACA repeats (5'-CACCACACCCACACACA-3') utilized in elongation of the TG-rich 3' chromosome end. Telomerase may alternate between two or more RNA templates during telomere synthesis (29). Est2 polymerase protein interacts with *TLC1* RNA via a conserved stem-

loop structural element as well as a small segment of residues located at the 5' end of the RNA (30) (Figure 5). Est1 binds directly to *TLC1* RNA (31), is a ssDNA-binding protein with specificity for telomeric sequences (32), and may be involved in recruitment and/or activation of the telomerase complex (33), possibly by utilization of an interaction with Cdc13 (34). Cdc13 binds TG-rich telomeric ssDNA and is involved in protection of telomeres and recruitment of the telomerase complex (35). The function of Est3 is not well elucidated, but it is thought to dimerize with itself (36) and interact with the N-terminal domain of Est2 (37).

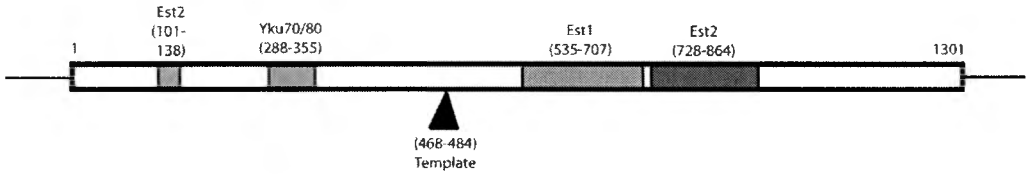

Figure 5. *S. cerevisiae TLC1* RNA protein binding regions.

The Ku complex, a heterodimer consisting of Yku70 and Yku80, is a DNA-binding protein thought to be the primary damage sensor in NHEJ. Ku has been found to bind both DNA ends in the early stages following formation of a DSB (38). Interestingly, there is a proposed binding site for Ku located on a 48-nt stem loop structural element of *TLC1* RNA (39) (Figure 5). Deletion of either of the Ku subunits results in loss of function for the complex, and these cells have multiple phenotypes including shortened telomeres, high temperature telomere instability that leads to cell death, and loss of transcriptional gene silencing near the telomeres (3).

Deletion of the *EXO1* gene, which encodes a 5′ to 3′ DNA exonuclease, rescues Ku deleted strains inviability at high temperature (37°C) and partially rescues the telomere length defect, indicating that Exo1 nuclease action is harmful to partially uncapped chromosome ends (40). Although Exo1 can act on uncapped telomeres, it is not normally thought to act at the chromosome ends (in part due to the presence of the Ku complex) but to substitute for the nuclease activity of the RMX complex at DSBs (12, 41).

TLC1 RNA was initially discovered by a screen of genes, that when overexpressed, would suppress the silencing of transcription normally present near the telomeres in *S. cerevisiae* (42). *TLC1* overexpression was also determined to rescue Ku mutant temperature sensitivity at 37°C (12, 43). It was later determined that overexpression of a 48-nt stem-loop of *TLC1* RNA, through an interaction with the Ku complex, was sufficient for disruption of telomeric silencing (39). Our laboratory has shown that in cells lacking RMX activity, overexpression of *TLC1* RNA increases cellular resistance to the DNA damaging agents *Eco*RI, MMS, and ionizing radiation (12, 44).

The primary goals of this project were to learn more about the mechanism by which elevated levels of telomerase are able to increase DSB repair and to increase our understanding of telomerase and telomeres in general and in relationship to DNA repair.

CHAPTER II

MATERIALS AND METHODS

I. MATERIALS

General Reagents

Ammonium sulfate (granular), sodium chloride, and sodium dodecyl sulfate (SDS) were purchased from Mallinckrodt AR (Paris, Kentucky). Agarose and ethidium bromide were purchased from Shelton Scientific, Incorporated (Shelton, CT). Hydroxyurea (HU) was purchased from US Biological (Swampscott, MA). Methyl methanesulfonate (MMS) was obtained from Fluka (Bucha, Switzerland). Tris base, lithium acetate dehydrate, calcium chloride, 99% glycerol, and polyethylene glycol were purchased from Invitrogen Life Technologies (Carlsbad, CA). Hygromycin B (HygB), ethylenediaminetetraacetic acid (EDTA), sodium citrate dehydrate, sodium hydroxide, and boric acid were obtained from EM (Darmstadt, Germany). Dimethyl sulfoxide (DMSO), Sarkosyl (N-lauroyl-sarcosine), Tween 20, and $MgCl_2$ were purchased from Sigma Chemical Co. (St. Louis, MO). G418 sulfate was purchased from Cellgro (Hardon, VA). 5-fluoroorotic acid (5FOA) used for selection of Ura^- cells was purchased from US Biological (Swampscott, MA). Maleic acid and formamide were obtained from Fisher Scientific Co. (Fair Lawn, NJ). Reagents used for immunodetection of Southern blots were all obtained from Roche Diagnostics Co. (Indianapolis, IN).

Enzymes and PCR reagents

Restriction enzymes, Klenow fragment and standard Taq DNA polymerases, and T4 DNA Ligase were purchased from New England Biolabs (Beverly, MA). Shrimp alkaline phosphatase (SAP) was purchased from USB (Cleveland, OH). Taq Plus Long, Herculase, and general PCR reagents were obtained from Stratagene (La Jolla, CA). ExTaq DNA polymerase was purchased from Takara (Madison, WI), and standard *Taq* DNA Polymerase was also purchased from Fermentas (Ontario, Canada).

Bacteriological and yeast media

All amino acids, plate agar, D-(+)-glucose, ampicillin, and galactose were purchased from Sigma. Difco bacto peptone, bacto yeast extract, bacto tryptone and bacto yeast nitrogen base dropout were purchased from Becton Dickinson Microbiological Systems (Sparks, MD).

Cell culture solutions and media

For general, non-selective growth, yeast cells were grown on YPDA (rich) media (1% bacto yeast extract, 2% bacto peptone, 2% glucose, 2% bacto agar, 0.001% adenine). In order to assess mitochondrial function, yeast cells were grown on YPG (1% bacto yeast extract, 2% bacto peptone, 2% bacto agar, 3% glycerol). Liquid media was prepared as plate media minus agar. For plasmid selection, yeast cells were grown on synthetic media with drop-out mix (0.17% yeast nitrogen base without amino acids or ammonium sulfate, 0.5% ammonium sulfate, 2% glucose or 2-3% galactose, 2% bacto agar, plus all essential amino acids minus the amino acids used for selection). YPGal

plates were made as described for YPDA, except with the substitution of 2-3% galactose for glucose. Plates with hydroxyurea (HU) were prepared by using appropriate media plus aliquots of a stock solution of 0.5 M HU solution mixed to obtain various concentrations of HU. Methyl methanesulfonate (MMS) plates were made using synthetic media, YPGal, or YPDA plus MMS mixed to obtain various concentrations. G418 sulfate and Hygromycin B were added to plates for selection of resistant strains at concentrations of 200 μg/ml and 250 μg/ml, respectively.

For propagation of *Escherichia coli*, cells were grown in LB + ampicillin (Amp) broth (1% bacto tryptone, 0.5% yeast extract, 0.5% NaCl, 0.01% ampicillin) or on LB + AMP plates (as broth, with 1.5% agar). *Escherichia coli* cells containing newly constructed plasmids were stored at -80°C in 15% (v/v) glycerol.

Yeast strains and plasmids

All yeast strains and plasmids used in this study are listed in Tables 1 and 2, respectively.

Table 1. Strains.

Strain	Genotype	Reference/Source
BY4742	*MATα his3Δ1 leu2Δ0 lys2Δ0 ura3Δ0*	45
T334	*MATα ura3-52 leu2-3,112 trp1· hisG reg1-501 gal pep4-3 prb1-1122*	12
VL6α	*MATα ura3-52 trp1(Δ63) lys2-801 his3-Δ200 met14 ade2-101*	46
S1InsE4A	*MATα ura3-52 leu2-3,112 trp1-289 his7-2 ade5-1 lys2.:InsE-4A*	47
UCC3505	*MATa ade2-101 his3-Δ200 leu2- Δ 1 lys2-801 trp1- Δ 63 ura3-52 ppr1:·HIS3 adh4. URA3-TEL-VIIL DIA5-1*	42
YLKL398	T334, Δ*his3*::[*GAL1p*::*EcoRI TRP1*] Δ*rad50· G418*^{r}	Lab strain
YLKL400	T334, Δ*his3*::[*GAL1p*::*EcoRI TRP1*] Δ*rad50*::*G418*^{r} Δ*rad52· LEU2*	Lab strain
YLKL503	VL6α, Δ*mre11·.G418*^{r}	12
YLKL529	S1InsE4A, Δ*mre11*::*G418*^{r}	48
YLKL615	VL6α, Δ*mre11*::*HygB*^{r} Δ*rad52*::*hisG*	Lab strain
YLKL650	BY4742, Δ*mre11 :G418*^{r}	Lab strain
YLKL652	BY4742, Δ*yku70.·HIS3*	Lab strain
YLKL801	T334, Δ*his3*::[*GAL1. EcoRI TRP1*] Δ*exo1*::*G418*^{r} Δ*rad50..hisG*	This study
YLKL802	T334, Δ*his3*::[*GAL1p*::*EcoRI TRP1*] Δ*dnl4 :G418*^{r} Δ*rad50:.hisG*	This study
YLKL804	UCC3505, Δ*mre11: HygB*^{r}	This study
YLKL813	BY4742, *trp1:.hisG-URA3-hisG*	This study
YLKL832	YLKL813, Δ*mre11:.G418*^{r}	This study
YLKL842	BY4742, *trp1..hisG*	This study
YLKL843	BY4742, Δ*yku70· HIS3 trp1..hisG*	This study

Table 2. Plasmids.

Plasmid	Description	Reference/Source
pCDNA50.3	*CEN/ARS URA3 GAL1p.:TLC1*	12
pRS314	*CEN/ARS TRP1*	49
pRS315URA3	*CEN/ARS URA3 LEU2*	This lab
pRS316	*CEN/ARS URA3*	49
pRS425	2μ *LEU2*	50
pVL459	2μ *URA3 CDC13*	51
pVL715	2μ *URA3 ADH1p:·EST2*	52
pVL735	2μ *URA3 ADH1p.·est2-D530A*	52
pVL743	2μ *URA3 ADH1p. est2-D670A*	52
pVL784	2μ *LEU2 ADH1p ·EST1*	52
pVL999	2μ *LEU2 ADH1p .EST2*	52
pRDK480	2μ *LEU2 ADH1p. EXO1*	53
pTRP61	2μ *TRP1 GAL1p::TLC1*	42
YEp-195-TEN1	2μ *URA3 TEN1*	54
YEp-195-STN1	2μ *URA3 STN1*	54
pTCG	2μ *TRP1 GAL1p*	39
pTCG 3XStem	2μ *TRP1 GAL1p:.TLC1*-3XStem	39
pTCG 3XStemMutant	2μ *TRP1 GAL1p··TLC1*-3XStem^{m}	39
pLKL64Y	2μ *LEU2 ADH1p· TLC1*	44
pLKL74Y	2μ *TRP1 GAL1p.:TLC1*	44
pLKL75Y	pLKL74Y, Δ(*Ecl136II-AflII)*	44
pLKL76Y	pLKL74Y, Δ(*Ecl136II-HpaI)*	44
pLKL77Y	pLKL74Y, Δ(*Ecl136II-NcoI)*	44
pLKL78Y	pLKL74Y, Δ(*BamHI-StuI)*	44
pLKL79Y	pLKL74Y, Δ(*BamHI-NcoI)*	44

Plasmid	Description	Reference/Source
pLKL82Y	*CEN/ARS GAL1-V10p⁻:EST2 URA3*	Thıs lab
pLKL83Y	2μ *ADH1p: TLC1 URA3*	This study
pLKL84Y	2μ *GAL1p .EST2 URA3*	This study
pCDNA50.3	*CEN/ARS GAL1p··TLC1 URA3*	12
YTCA-1	$TG_{(1-3)}$ repeat plasmid	55

II. METHODS

Chromosomal and plasmid DNA purification

Yeast chromosomal DNA was purified following the manufacturer protocol using MasterPure™ Purification Kit by Epicentre Technologies (Madison, WI). High purity chromosomal DNA for some experiments involved additional purification using a Qiagen Spin Column Miniprep Kit (Maryland, VA). Plasmid DNA was purified using a rapid boiling lysis method (56).

Yeast transformations

Transformations of yeast cells were completed using either a high efficiency lithium acetate method described by Gietz *et al.* (57) or a rapid lithium acetate and DMSO-based transformation method by Soni *et al.* (58).

E. coli transformations

Transformations of *E.coli* cells were completed using a method derived from Miller and Chung (59).

Gel electrophoresis

Gel electrophoresis was performed using 0.6-1.2% agarose gels in TBE (90 mM tris-borate, 2 mM EDTA) running buffer in a Life Technologies Horizon 11-14 gel rig at a constant voltage of 110 V. Gels were stained with ethidium bromide and gel images were captured using a Kodak IS440 CF imaging system with Kodak 1D imaging software.

Polymerase Chain Reaction

PCR was performed in an Applied Biosystems 2720 Thermal Cycler for 28-32 cycles. Denaturation was set at 94°C or 95°C for 30 seconds, annealing temperatures ranged from 38-48°C for 40 seconds, and extension temperature was 72°C for 60-120 seconds.

Southern Blots

PCR amplification of nonradioactive DIG probe. Probes for Southern analysis were synthesized by PCR with *Taq* polymerase using M13 forward primer (5′-AGCGCGCAATTAACCCTCACTAAAG-3′), M13 reverse primer (5′-CAGGAAACAGCTATGACC-3′), 10X PCR DIG labeling mix (2 mM dATP, 2 mM dCTP, 2 mM dGTP, 1.3 mM dTTP, 0.7 mM digoxigenin-11-dUTP).

DNA isolation and purification. Overnight cultures were grown in selective liquid media in a 30°C shaker. After purification, DNA concentrations were quantified on a Hoefer DyNA Quant 200 Fluorometer (Amershem Pharmacia Biotech) as described by the manufacturer. Three μg of DNA was digested overnight with *Xho*I at 37°C. The *Xho*I-digested DNA was concentrated by ethanol precipitation and again quantified by fluorometry. One μg of each sample was loaded onto a 1.2% agarose gel and visualized using ethidium bromide.

Denaturation and neutralization. After electrophoresis, the gel was washed with denaturation buffer (8.7% sodium chloride, 2% sodium hydroxide) for a total of 35 minutes at room temperature. Next, the gel was washed in neutralization buffer (8.7% sodium chloride, 6.1% Tris base) for 35 minutes at room temperature. The DNA from

the gel was transferred overnight onto an N^+ Hybond membrane using a homemade capillary transfer apparatus. Once overnight transfer was complete, the DNA was crosslinked to the membrane in a UV-Stratalinker 2400 (Stratagene) at 120,000 microjoules for 20 seconds.

Hybridization. For prehybridization, the membrane was washed twice in a glass roller bottle in 15 mL of prehybridization/hybridization solution (50% v/v formamide, 5X SSC, 0.1% sarkosyl, 0.02% SDS, 1X blocking agent from Roche) for one hour at 40°C. SSC buffer (5X) was prepared from 20X SSC stock solution (35.1% NaCl and 17.6% sodium citrate). Thirty microliters of digoxigenin (DIG)-labeled probe (2 µL probe/mL hybridization buffer) was added to the membrane and rolled overnight at 40°C.

Detection by chemiluminescence. The blot was washed twice with 2X SSC/0.1% SDS and shaken at room temperature for five minutes. The blot was then washed twice for five minutes each in 2X stringency wash solution (0.1M maleic acid, 0.15 M NaCl, 0.3% Tween 20 v/v; pH 7.5). Next, the blot was equilibrated for one minute in wash buffer, which was poured off and replaced with fresh wash buffer. After another minute, the wash buffer was poured off and 100 mL of blocking solution was added, allowing the blot to shake in it for 30 minutes. The blocking solution was then removed, and enzyme-linked antibody solution (4 µL antibody solution from Roche in 20 mL 1X blocking solution) was added, and the blot was left to shake for 30 minutes. The antibody solution was poured off and the blot was washed twice with 100 mL wash buffer for 15 minutes each. This solution was poured off and the blot was incubated for 2-5 minutes with 20 mL of detection buffer (0.1M Tris-Hcl, 0.1 M NaCl; pH 9.5). The blot was removed from the buffer and placed into a plastic bag where 1 ml of substrate solution containing

disodium 3-{4-methoxyspiro(1,2-dioxetane-3,2'-(5'-chloro)tricyclo[3,3.1.13.7]decan}-4-yl) phenyl phosphate (CSPD), from Roche Diagnostics was added directly onto the blot in the bag. The bag was immediately closed and the substrate solution was spread evenly over the surface of the membrane. The membrane sat at room temperature for five minutes before all of the liquid was squeezed out of the bag and the bag was sealed. The blot was then incubated at 37°C for 10 minutes. For imaging, the blot was placed in an X-ray cassette and with one sheet of 8x10 cm Kodak Biomax MR film. Exposure times for each film varied from 10-120 minutes before development.

Dilution pronging cell survival assays

Cells were harvested into sterile deionized H_2O, diluted 1/40, sonicated for 8-10 seconds at 3 watts using a Sonics Vibracell Ultrasonic Processor (Newtown, CT), and then quantitated using a Reichert (Buffalo, NY) hemocytometer on a Comcon (Russia) LOMO phase contrast microscope. To a sterile 96-well microtiter dish, yeast cells were added to a cell titer of $0.5x10^7 - 5x10^7$ cells per 220 µl (total volume ~220 µL per well). Next, a series of 5-fold dilutions of the cells were made along the length of the dish using a multi-pipettor. The cells were then pronged onto control plates a ⊿ onto plates containing either varying concentrations of DNA damaging agents (*e.g.,* MMS, HU), media containing 0.05-0.2% galactose for the induction of *Eco*RI endonuclease, or in the case of Δ*yku70* mutants, plates to be incubated at 38°C. All wild-type and repair-deficient cells, with the exception of Δ*yku70* cells tested for temperature sensitivity, were grown at 30°C and analyzed after 2-6 days growth. Images of plates were captured using a Canon Powershot G3 digital camera and saved as JPEG format files.

Plasmid clonings

pLKL83Y (2μ ADH1p::TLC1 URA3). pCDNA50.3 (12) was digested with *Bam*HI and *Ecl*136II in KGB buffer (100 mM potassium glutamate, 25 mM Tris-acetate (pH 7.6), 10 mM magnesium acetate) to release the ~1.3 kb *TLC1* gene fragment, filled in using Klenow DNA polymerase and dNTPs as recommended by New England Biolabs, and then gel purified from a 0.55% agarose gel. pVL715 was cut with *Hind*III in KGB buffer to remove the *EST2* gene, and the vector portion was filled in using Klenow, phosphatased using shrimp alkaline phosphatase (SAP) to prevent plasmid recircularization, and gel purified. The gel purified fragments were ligated together using T4 DNA Ligase at an approximate ratio of 10:1 (insert:vector) using 50 ng of vector and 100 ng insert. The resulting ligation mix was transformed into TOP10 competent *E. coli* (Invitrogen) and allowed to propagate at 37°C on LB + Amp plates. Plasmid DNA from individual *E. coli* colonies was isolated and verified on a 0.7% agarose gel. Plasmids determined to be a larger size than the recircularized vector underwent restriction mapping verification of insert uptake orientation. A functional test of *TLC1* RNA overexpression was performed by transformation of pLKL83Y into Δ*mre11* cells and subsequent exposure to *Eco*RI induced DNA damage. Rescue of DNA damage in RMX-deficient cells by overexpression of *TLC1* RNA provided confirmation of pLKL83Y function.

pLKL84Y (2μ GAL1p::EST2 URA3). pLKL82Y *(CEN/ARS GAL1-V10p:.EST2 URA3)* was digested with *Bam*HI and *Not*I in KGB buffer to release the *EST2* gene fragment, which was then gel purified on a 0.55% agarose gel. The vector pTCG (a generous gift from Dan Gottschling) was digested with *Bam*HI and *Not*I, and then

phosphatased using SAP, and later purified using a Qiagen Spin Column Miniprep Kit. The resulting purified DNA fragments were then ligated using T4 DNA Ligase at an approximate ratio of 10:1 (insert:vector) using 50 ng of vector and 100 ng insert. The resulting ligation mix was transformed into TOP10 competent *E. coli* and allowed to propagate at 37°C on LB + AMP plates. Plasmid DNA preps from individual *E. coli* colonies were then isolated and verified on a 0.7% agarose gel. Plasmids determined to be a larger size than pTCG underwent restriction mapping to verify orientation of insert with respect to the vector promoter sequence. Plasmids that were verified using restriction mapping were then transformed into Δ*yku70* cells and grown at 38°C. Rescue of Δ*yku70* temperature sensitivity by overexpression of *EST2* provided functional verification of Est2 protein production by pLKL84Y.

Yeast strain construction

Strains containing *Δrad50::hisG* and *trp1::hisG* were created by plating the parent strains containing the *hisG-URA3-hisG* cassette to 5-FOA plates that counter selected for cells undergoing recombination events that resulted in deletion of the *URA3* gene.

YLKL804 (Δ*mre11::HygB*^{r}). *YLKL832 (trp1::hisG-URA3-hisG* Δ*mre11::G418*^{r}). The gene for HygB-resistance from the plasmid pAG32 (60) was PCR amplified using 5′gmre11 (GGACTATCCTGATCCAGACACAATAAGGATTTTAATTACTACAGA CGTACGCTGCAGGTCGAC) and 3′gmre11 (GGAAGGAATCTAGCCCATTACCATTGAATGCGAAATTTGTCTCAT ATCGATGAATTCGAGCTCG) primers. This amplification created DNA fragments

containing the HygB-resistance gene with homology at its 5′ and 3′ ends to the 5′ and 3′ ends of the chromosomal *MRE11* gene. This DNA fragment was transformed into the parent yeast strain (UCC3505) and colonies were selected for HygB resistance. Chromosomal DNA was then purified, and HygB-resistant isolates were verified for disruption of the *MRE11* gene by comparison of DNA fragment size from PCR reactions of *MRE11*+ controls and HygB-resistant isolates using primers that flanked the 5′ and 3′ ends of the *MRE11* gene sequence using the primers 5′mre11 (AGTATGGCCAATCGAATAGAACCCAA) and 3′mre11 (TACGAACAAAAGAGCAAAGGCTGGAA).

YLKL813 (trp1::hisG-URA3-hisG). Disruption of the *TRP1* gene was accomplished by transformation of pNKY1009 (*trp1::hisG-URA3-hisG*) (61) into the parent strain BY4742. Resulting Ura^+ colonies were verified to have disrupted the *TRP1* gene by lack of growth on Glucose – Trp synthetic plates.

YLKL832 (trp1::hisG-URA3-hisG Δmre11::G418^r). The gene for G418-resistance from the plasmid pFA6MX4 (62) was PCR amplified using 5′gmre11 and 3′gmre11 primers. This amplification created DNA fragments containing the G418-resistance gene with 5′ and 3′ end homology with the 5′ and 3′ ends of the chromosomal *MRE11* gene. This DNA fragment was transformed into the parent yeast strain (YLKL813) and colonies were selected for G418 sulfate resistance. Chromosomal DNA was purified from G418-resistant isolates and verified for disruption of the *MRE11* gene by comparison of DNA fragment size from PCR reactions of *MRE11*+ controls and G418-resistant isolates using the primers 5′mre11 and 3′mre11.

CHAPTER III

RESULTS AND DISCUSSION

This research project focused on components of telomerase, particularly the RNA template component *TLC1,* with some emphasis on the polymerase subunit, Est2. Of particular interest was the mechanism by which increasing cellular levels of telomerase components is able to increase DNA damage resistance of cells lacking the Rad50/Mre11/Xrs2 (RMX) complex. A previous study screened for cDNAs that when overexpressed alleviated the MMS-sensitivity of RMX mutants, and the screen yielded two genes, *EXO1* and *TLC1* (12). The mechanism by which Exo1 rescues was reasonably elucidated, as described in that paper. However, the mechanism of repair induced by *TLC1*, the RNA subunit of telomerase, remained unknown. Phenotypes of *TLC1* RNA overexpression in yeast cells include: rescue of X-ray and MMS-induced DNA damage in RMX mutants, disruption of telomeric silencing (55), and rescue of the Ku high temperature lethality observed in *yku70* and *yku80* mutants (12, 43, 63,). Experiments herein focused primarily on *TLC1* RNA and Est2 and understanding the mechanisms involved in stimulation of DSB repair.

Overexpression of TLC1 RNA or Est2 has no effect on telomere length in RMX mutants

Overexpression of *TLC1* RNA rescues the X-ray and MMS-sensitivity of RMX mutants. The RMX complex plays a role in maintenance of telomeres, and RMX-defective mutants have shortened telomeres when compared to wild-type cells (3). As the primary function of telomerase is extension of telomeres, it was hypothesized that overexpression of *TLC1* RNA or Est2, the polymerase subunit of telomerase, might rescue DNA damage in RMX mutants due to telomere stabilization and elongation. In collaboration with a previous graduate student, Shanna Calero, genomic DNA was purified, digested with *Xho*I, separated by electrophoresis, and then a Southern blot was performed (see Methods) to analyze telomere length in *mre11* cells (YLKL650) overexpressing *TLC1* RNA (pLKL64Y) or Est2 (pVL999) (Figure 6).

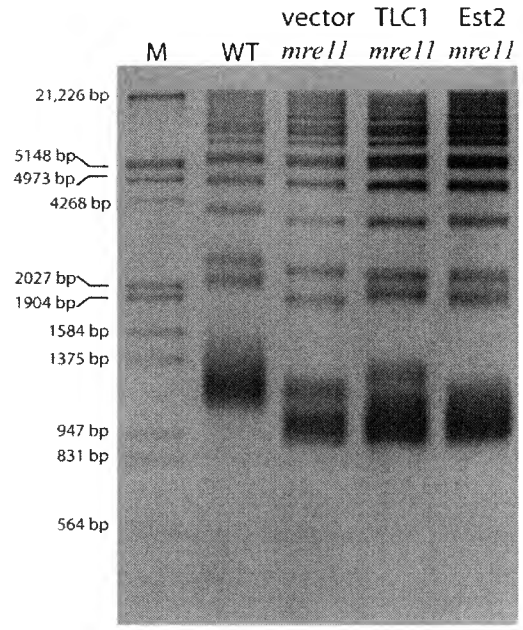

Figure 6. Southern blot analyzing effects of overexpression of *TLC1* RNA or *EST2* on telomere length. M = molecular weight markers, WT = wildtype BY4742

The restriction endonuclease *Xho*I cuts ~1200 bp from the ends of most yeast chromosomes in wildtype cells producing a broad band when probed with a telomeric DNA fragment (the lowest band in the lane labeled "WT"). In *mre11* cells the corresponding band migrated lower at ~1000 bp due to a loss of telomere length. Overexpression of *TLC1* RNA or Est2 protein had no noticeable effect on telomere length in the *mre11* cells. The cells were not subjected to DNA damage, so these results do not rule out rescue of DNA damage in RMX-defective cells by telomerase activity, such as the potential for *de novo* telomere addition at broken DNA ends.

Telomere silencing

Genes located within several thousand base pairs of a chromosome end are transcriptionally repressed, a phenomenon called telomeric silencing. In the strain UCC3505, the positioning of *URA3* near the telomere of chromosome VIIL (the left end of chromosome seven) causes the gene to be transcriptionally repressed under normal conditions (effectively *ura3*$^-$). Overexpression of *TLC1* RNA has been shown to disrupt telomeric silencing, allowing for cells that normally exhibit a *ura3*$^-$ phenotype to become *URA3*$^+$. These assays were conducted by Singer *et al.* using media containing 5-fluoroorotic acid (5-FOA) (42). 5-FOA is toxic to cells with a functional *URA3* gene encoding orotidine 5'-monophosphate decarboxylase (64) and therefore only cells that are silenced (*ura3*$^-$) can grow on plates containing this drug.

TLC1 overexpression disrupts telomere silencing in wildtype cells, but its impact on DNA repair-deficient strains has not been previously investigated. To determine if overexpressing telomerase components has a similar effect on RMX mutants, first an appropriate strain was constructed. PCR-mediated gene disruption of the *MRE11* gene in the strain UCC3505 (YLKL564) was conducted using HygB (see Methods for full description). Into the resulting strain (YLKL804) and the parent strain (YLKL564), control vector pRS315, pLKL64Y (ADH1p::*TLC1*), pVL999 (ADH1p::*EST2*), or pVL784 (ADH1p::*EST1*) was transformed. Cells were then patched onto 5-FOA-Leu plates and taken from these patches and 5-fold serial dilution pronged onto plates containing 5-FOA. Results are seen in Figure 7.

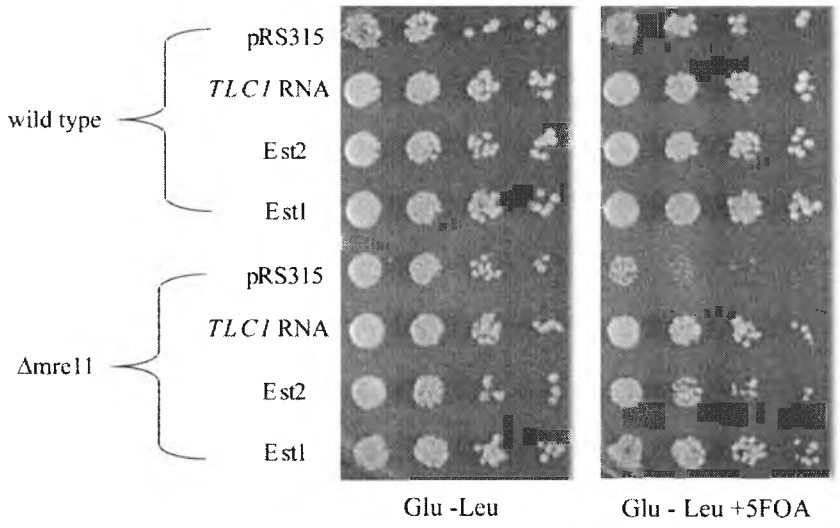

Figure 7. Effect of overexpressing telomerase components on telomere silencing. Overexpressing telomerase components had no effect on *URA3* telomere silencing in UCC3505 (wildtype cells). In *mre11* cells, overexpression of either *TLC1* RNA, Est2, or Est1 appeared to restore most cells to a silenced state. Approximately 10^7 cells were serially diluted five fold and pronged.

With the strain UCC3505, previous studies showed that overexpression of *TLC1* RNA disrupts telomere silencing, causing the *ura3*$^-$ cells to become *URA3*$^+$ and therefore 5-FOA-sensitive. In our experiments, no inhibition of growth is seen that would be caused by disruption of *URA3* silencing allowing for cells to become *URA3*$^+$ and vulnerable to 5-FOA. RMX mutants have been shown to have normal silencing (65). However, again our results conflict with the previously published data. Of note, our RMX mutant cells appear to have disrupted telomere silencing (many *URA3*$^+$ cells), but when *TLC1* RNA, Est2, or Est1 are overexpressed, there is a restoration of silencing (i.e., there are more *ura*$^-$ cells that can grow on the 5-FOA plates). The source of this discrepancy might be due to patching cells to 5-FOA before pronging. This could impose

selection for silenced cells (even if in the case of *TLC1* RNA overexpression, the percentage of silenced cells is low) and then only these selected cells are used subsequently, as opposed to using the entire population of both silenced and unsilenced cell states. These experiments clearly demonstrate an effect of telomerase overexpression on transcription near telomeres in *mre11* mutants. However, since we were unable to reproduce the original observation of Singer *et al.* in wildtype cells in our lab, the phenomenon was not studied further.

TLC1 RNA-mediated repair of bleomycin and HU-induced damage is dependent on homologous recombination

A previous graduate student in this laboratory, Jared Cassiano, determined that overexpression of *TLC1* RNA in RMX mutants required the recombination pathway but not the NHEJ pathway to suppress MMS-induced killing (44). Homologous recombination, the primary repair pathway in *S. cerevisiae*, involves the *RAD52* epistasis group which includes the RMX complex. Deletion of *RAD52* causes a strong reduction in recombination. Previous studies of *TLC1* rescue of DNA repair focused on MMS and gamma ray-induced damage. To investigate this further, the ability of *TLC1* to rescue damage induced by two very different mutagens, bleomycin and hydroxyurea (HU) was assessed. The role of Rad52 was also investigated. MMS causes methylation of guanine and adenine bases to form 7-methylguanine and 3-methyladenine, respectively (66). This damage can result in base mispairing or halted DNA replication, both of which are repaired by base excision repair (BER). BER can produce SSBs that if not properly repaired may result in DSBs in replicating DNA (67). HU inhibits the enzyme

ribonucleotide reductase, which causes a depletion of nucleotides and results in DNA double-strand breaks near stalled replication forks (68). Bleomycin, a drug commonly used in chemotherapeutic techniques, functions via a free radical-driven mechanism requiring Fe(II) and oxygen to generate lesions similar to those induced by ionizing radiation (e.g., abasic sites, single-strand breaks containing 3' groups that stall DNA replication and DSBs with damaged ends) (69, 70).

A 5-fold serial dilution pronging of YLKL503 (*mre11*) cells and YLKL615 (*mre11 rad52*) cells containing control vector pRS315 or pTRP61 (*GAL1p::TLC1*) was performed to analyze overexpression of *TLC1* RNA in the presence of bleomycin and HU-induced damage (Figure 8). MMS-containing plates were included as a control.

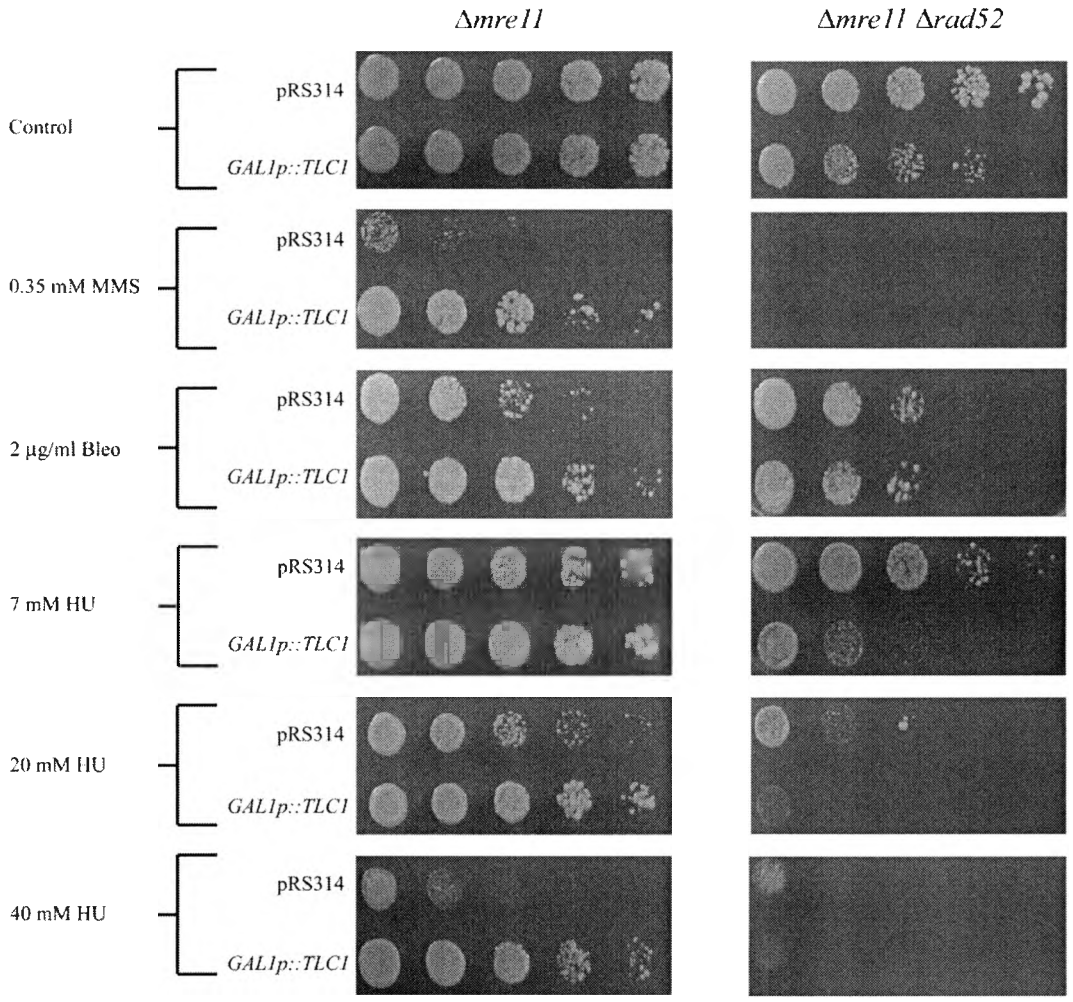

Figure 8. Effect of *TLC1* RNA on MMS, bleomycin, and HU-induced killing in *mre11* and *mre11 rad52* mutants. Overexpression of *TLC1* RNA suppresses MMS and HU (and to a lesser extent, bleomycin)-induced killing in *mre11*, but not in *mre11 rad52* double mutants. Cells were serially diluted 5-fold as in Figure 7.

As seen previously, overexpression of *TLC1* RNA rescued MMS-induced damage in *mre11* cells, but was unable to rescue *mre11 rad52* cells that lack recombination (Figure 8, second row). The double mutant *mre11 rad52* cells were also not rescued at

lower doses of MMS (44). *TLC1* RNA overexpression in *mre11 rad52* cells exhibited a slight toxicity without the addition of any drug (Figure 8, top right). Bleomycin-induced killing was rescued slightly by *TLC1* RNA overexpression in *mre11* cells but not in *mre11 rad52* cells. In *mre11* cells the bleomycin results appear to somewhat correlate with results previously published (12) where *TLC1* RNA overexpression displayed only a modest rescue of ionizing radiation, as bleomycin is proposed to mimic ionizing radiation. When HU was present, *TLC1* RNA overexpression exhibited a phenotype similar to when MMS was present in that there was rescue of *mre11* cells but not of *mre11 rad52* cells. These results suggest that Rad52-mediated homologous recombination is also required for *TLC1* RNA suppression of bleomycin or HU-induced damage in RMX-deficient cells.

Analysis of deletion derivatives of TLC1 RNA

Most *TLC1* RNA overexpression studies in our laboratory have utilized the entire 1301 bp *TLC1* gene. With this in mind, former graduate student Jared Cassiano constructed several plasmids that could express derivatives of *TLC1* RNA containing truncated portions of the gene (44). The aim was to determine what sections of the RNA might be required for enhancement of repair of DNA damage in RMX mutants though these initial experiments were unsuccessful because of the strains used. As seen in Figure 9A, *TLC1* RNA has several features, including the template region and predicted binding sites for different telomeric proteins. In Figure 9B several deletion derivatives are shown. Three of these derivatives had increasing amounts of the 3' end deleted (pLKL75-77Y) and the other two contained deletions of the 5' end (pLKL76-77Y).

These plasmids along with a wildtype *TLC1* RNA expression plasmid (pLKL74Y) were transformed into YLKL529 (*mre11*) cells, and then pronged onto plates containing no drug, MMS or HU.

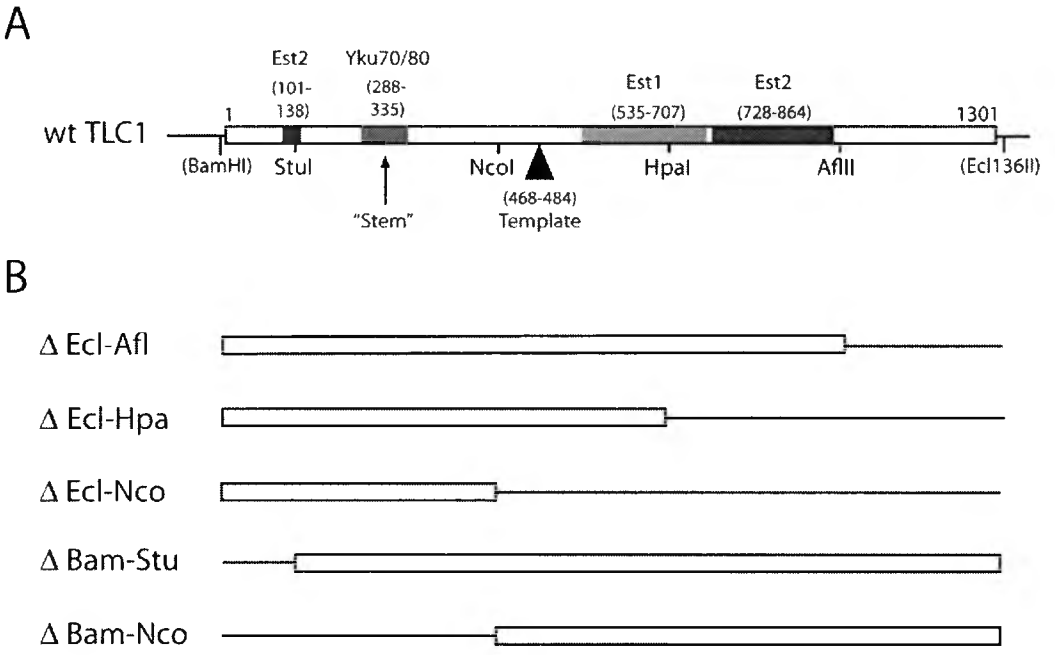

Figure 9. Deletion derivatives of *S. cerevisiae TLC1* RNA. A – *TLC1* RNA protein binding regions and unique restriction sites. B – Deletion fragments of *TLC1* RNA. White rectangles indicate portions retained in the constructs. Overexpression plasmids containing truncated genes were pLKL75Y (ΔEcl-Afl), pLKL76Y (ΔEcl-Hpa), pLKL77Y (ΔEcl-Nco), pLKL78Y (ΔBam-Stu), and pLKL79Y (ΔBam-Nco).

As seen in Figure 10, both MMS and HU-induced DNA damage were rescued by the overexpression of *TLC1* RNA as seen before (second row). Notably, all *TLC1* RNA

deletion derivatives except for the ΔBam-Nco mutant were able to increase resistance to the drugs. Analyzing the similarities of the deletion derivatives, all of the RNAs that rescued repair contained the stem loop region where binding of the Ku complex (Yku70 and Yku80) occurs (see Figure 9A). The deletion derivative unable to rescue (ΔBam-Nco) was the only fragment that did not contain the stem loop region. This evidence suggests a requirement for Ku binding by *TLC1* RNA for repair of DSBs in RMX mutants.

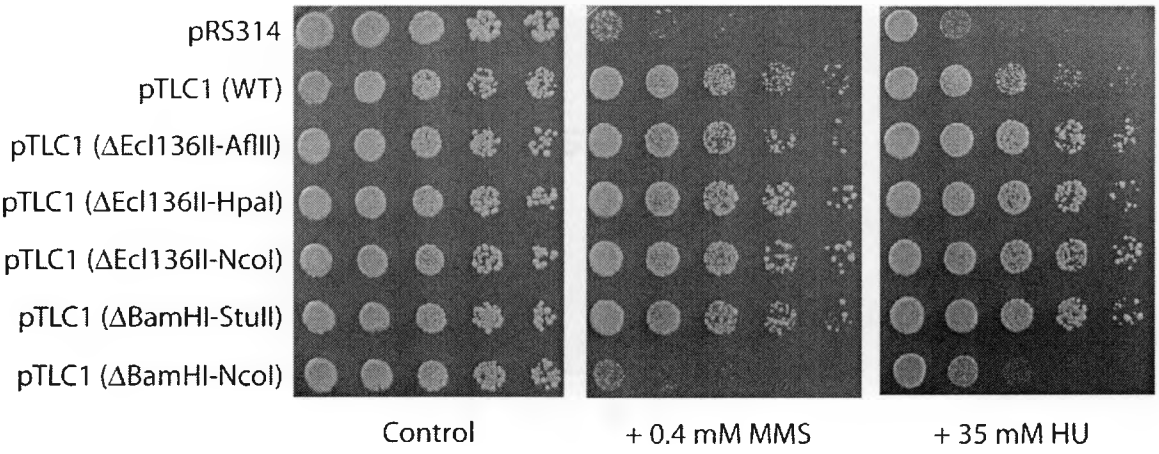

Figure 10. Effect of *TLC1* RNA deletion derivatives on MMS and HU-induced DNA damage in *mre11* cells. Overexpression of wildtype *TLC1* RNA and all deletion derivatives except ΔBamHI-NcoI rescues MMS and HU-induced DNA damage of *mre11* cells.

Analysis of overexpression of the TLC1 stem-region

Previous work by Dan Gottschling's lab revealed a 48 nt stem-loop structure (nt 288-335) within the 1.3 kb *TLC1* RNA that interacts with the Yku80 protein (39). Overexpression of a gene containing three tandem copies of the 48 nt stem loop disrupted

telomeric silencing, a phenotype of wildtype *TLC1* RNA overexpression, better than overexpression of one copy of the stem region. As a phenotype of *ku*$^{-}$ cells is also loss of telomeric silencing, Gottschling suggested that overexpression of *TLC1* RNA caused the cells to become effectively Ku^{-} at the telomeres because Yku70 and Yku80 proteins were bound to the RNA molecules.

The *TLC1* deletion derivatives experiment suggested a requirement for the 5' end of *TLC1* for repair of DNA damage in RMX mutants, possibly because of a requirement for the Ku-binding region. To further evaluate this premise, it was necessary to construct a BY4742 strain that was *trp1* and Δ*mre11* (YLKL832, see Methods). Once the strain was constructed, pRS314, pTRP61 (*TLC1*), or pTLC1-3XStem (containing three copies of the 48 nt stem sequence) was transformed into YLKL832 (*mre11*). The resulting transformants were pronged onto galactose minus tryptophan plates containing no drug, or the same plates with MMS or HU (Figure 11). As seen in the figure, overexpression of the stem region of *TLC1* RNA (rows three and four) was sufficient to rescue both MMS and HU-induced killing of *mre11* cells.

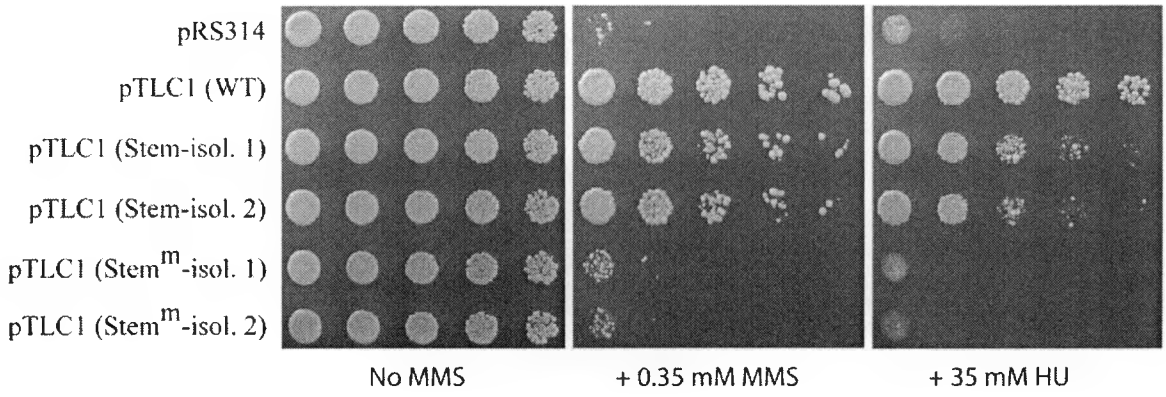

Figure 11. Effects of the *TLC1* RNA 3x-stem region on MMS and HU-induced lethality in *mre11* mutants. Overexpression of *TLC1* RNA or the 3x-Stem region was able to rescue MMS and HU-induced lethality. Overexpression of the 3x-Stem mutant was not able to rescue killing by either MMS or HU.

The Ku complex is highly conserved from yeast to humans. *TLC1* RNA interaction with Ku is also conserved, as the human Ku protein has been shown both *in vivo* and *in vitro* to interact with the RNA component of human telomerase via a region structurally similar to the yeast stem region (71). Figure 12 shows a sequence alignment using ClustalW with *TLC1* 5' end sequences from several *Saccharomyces* species including *S. kudriavzevii, S. mikitae, S. cariocanus, S. paradoxus,* and *S. cerevisiae*.

In the figure, which shows nt 232-411 of *S. cerevisiae* (out of 1301 nt), positions that are 100% conserved are shown in black. The stem region of *TLC1* RNA of *S. cerevisiae* (shown in blue, sequence underneath the alignment) is highly conserved. Positions shown in maroon are point mutations (T301A, T307G, T324G) in the stem mutant that, together, have been shown to cause Ku to be unable to bind *TLC1* RNA in gel-shift assays (72). Importantly, all three nt that were changed are found in the large,

conserved block from nt 294-324. Thus, the mutations in the stem loop mutant are within this highly conserved sequence of this proposed stem structure, and this mutant RNA is unable to bind Ku80 protein in *in vitro* assays.

To determine the importance of Yku80 binding to the stem region, a derivative of the pTLC1-3XStem plasmid was tested that had all three mutations. The ability of this plasmid (pTLC1-3XStem^{m}) to rescue *mre11* mutants was assessed. As shown in Figure 12 (bottom two rows), overexpression of the mutant stem RNA was unable to increase resistance to HU or MMS. This result strongly suggests that *TLC1* RNA-mediated repair involves binding to the Ku complex.

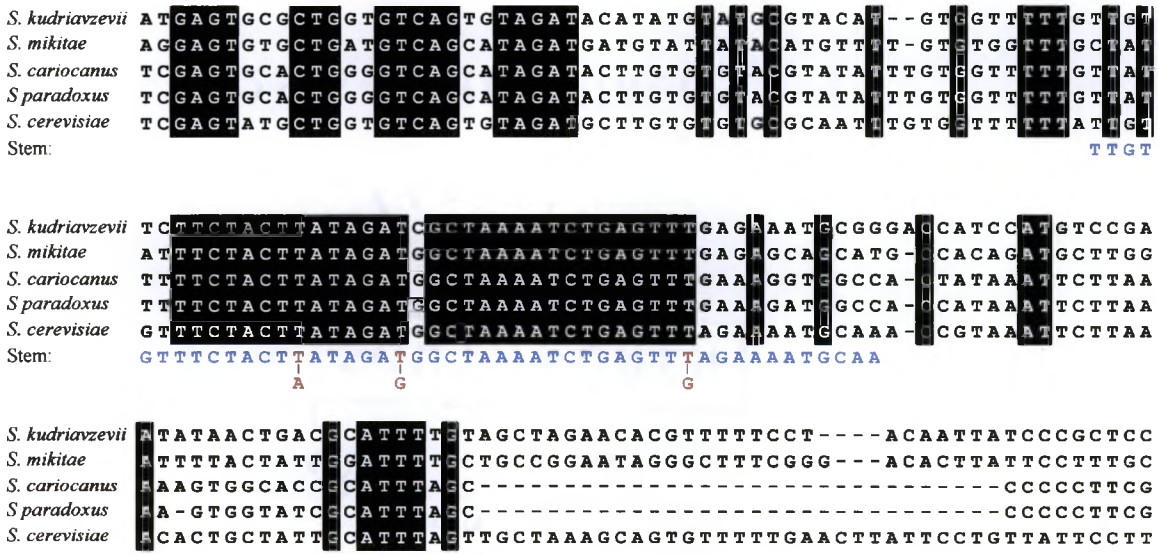

Figure 12. Sequence alignment containing the stem region of the *TLC1* gene. Sequence alignment of a portion of the *TLC1* gene (*S. cerevisiae* 232-411) including the stem loop region (288-335 in *S. cerevisiae*) shown in blue, as defined by Gottschling (39). The positions of the mutations in the stem loop mutant are shown in maroon (T301A, T307G, T324G).

A model for TLC1 RNA titration of Ku from DSBs in RMX cells

Our laboratory has shown that when subjected to MMS or HU-induced damage, RMX mutants overexpressing the telomerase RNA template component *TLC1* are able to rescue growth inhibition. It has also been found that the homologous recombination pathway of DSB repair is required and the NHEJ pathway is not. In addition to *RAD52*, it was also observed previously that the 5' to 3' exonuclease Exo1 is essential (44). The stem loop region of the *TLC1* RNA is required for repair and this region's ability to interact with the Ku complex has been shown to be of vital importance for rescue. Utilizing this data, we propose a model where overexpression of *TLC1* RNA in RMX mutants titrates the Ku complex away from DSBs-induced by MMS or HU, allowing better access for repair by the backup nuclease Exo1 and/or the recombination machinery of the cell. This model, which is described in more detail later, could also explain the toxicity to *mre11 rad52* cells when *TLC1* RNA is overexpressed. Titration of Ku would make the cells effectively *mre11 rad52 ku*$^{-}$; cells that are both *yku70* and *mre11* experience telomere degradation and are inviable (73), and this could be the source of growth inhibition.

Telomerase components can mediate repair of EcoRI-induced DSBs in both NHEJ- and recombination-deficient cells

To provide further insight into the mechanism of telomerase-mediated DNA repair in RMX-defective cells, the bacterial restriction endonuclease *Eco*RI was utilized. In contrast to the mechanisms of bleomycin, HU, or MMS, the endonuclease *Eco*RI causes damage to DNA via DSBs only. *Eco*RI is a restriction endonuclease that

recognizes and cleaves the dsDNA sequence G$^{\downarrow}$AATTC at the 3' end of the guanine on both strands. This produces a sticky-ended double-strand break containing complementary ends. This laboratory had previously determined that overexpression of *TLC1* RNA can enhance repair of *Eco*RI-induced DSBs in RMX mutants. Interestingly, initial tests determined that high expression levels of Est2 polymerase also rescue *Eco*RI-induced killing, but does not appear to rescue MMS-induced damage (74). Initial studies of Est2 overexpression were conducted using a *CEN/ARS* (single copy) plasmid with an *ADH1* promoter. *ADH1p* is a strong constitutive promoter. As *TLC1* RNA was expressed using 2 μ (high copy number) plasmids with the very strong *GAL1* promoter to rescue MMS-induced killing, it was considered a strong possibility that our first Est2 expression plasmid simply didn't make enough Est2 protein to rescue MMS-sensitivity.

An Est2 plasmid containing the features of the *TLC1* vectors was created, as shown in Figure 13 (pLKL84Y, see Methods) to determine if differences in expression level could account for the lack of repair of MMS-induced damage. As indicated earlier, the 2μ circle origin of replication confers high copy number on the plasmid (~50 per cell), and *GAL1p* is a strong galactose-inducible promoter. Upon testing, pLKL84Y, containing improved expression levels of Est2 was still unable to rescue MMS-induced damage in RMX-deficient cells (data not shown).

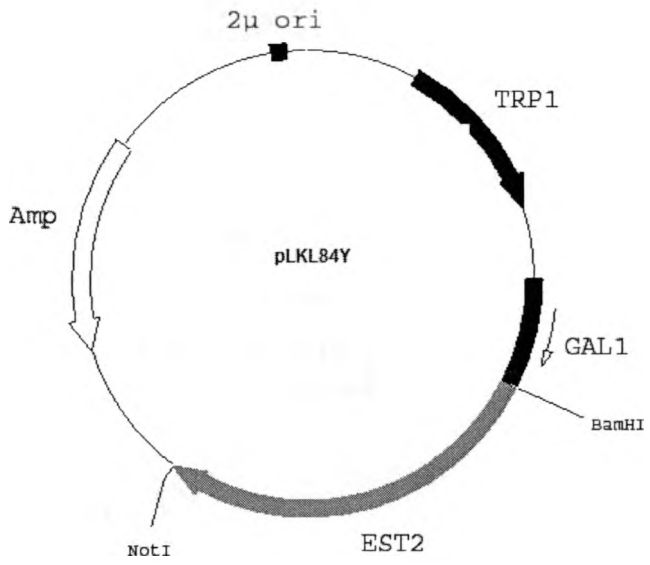

Figure 13. Plasmid map of pLKL84Y. Graphical representation of plasmid pLKL84Y containing a 2μ origin of replication and *GAL1p::EST2*.

In addition to Est2 polymerase, graduate student Shanna Calero previously demonstrated that overexpression of the telomerase-associated protein Ten1, but not another called Stn1, could rescue *Eco*RI-killing but not MMS (74). Since different components of the telomerase complex (*TLC1* RNA, Est2, and Ten1) differentially rescue various forms of DNA damage, it was conceivable that different mechanisms were involved. To determine the DSB repair pathway requirements of *Eco*RI-induced damage of RMX cells, control vector (pRS316), *TLC1* RNA (pLKL83Y), Est2 (pVL715), or Ten1 (YEP195-Ten1) was transformed into Δ*rad50* (YLKL398), Δ*rad50* Δ*rad52* (YLKL400), Δ*rad50* Δ*dnl4* (YLKL801), and Δ*rad50* Δ*exo1* (YLKL802) strains containing *GAL1p*::*Eco*RI integrated onto a chromosome. Cells were pronged onto

glucose media or glucose media containing galactose for induction of the *GAL1p::Eco*RI cassette on the chromosome (Figure 14).

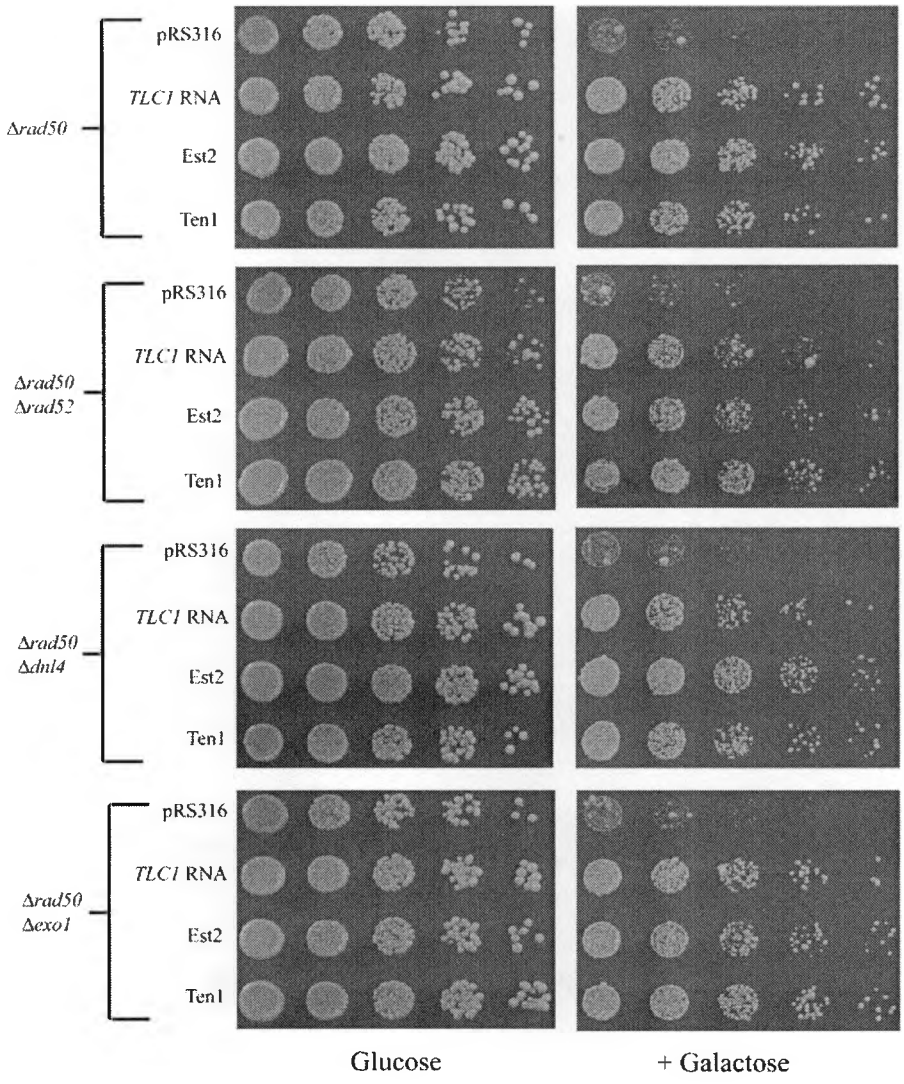

Figure 14. Overexpression of *TLC1* RNA, Est2, or Ten1 in Δ*rad50*, Δ*rad50* Δ*rad52*, Δ*rad50* Δ*dnl4*, and Δ*rad50* Δ*exo1* mutants. Cells on glucose (control) or with galactose present (causing induction of *Eco*RI).

As shown in the figure, galactose-induced expression of *Eco*RI was lethal in each of the DNA repair-deficient strains that contained only the plasmid vector pRS316. In contrast, plasmids expressing *TLC1* RNA, Est2, or Ten1 were all capable of rescuing *Eco*RI-induced damage in *rad50*, *rad50 rad52* (recombination-deficient), *rad50 dnl4* (NHEJ-deficient), and *rad50 Δexo1* cells. These results are strikingly different from data found with MMS, bleomycin, or HU-induced damage, where cells overexpressing Est2 were unable to rescue, and *TLC1* RNA required the recombination pathway for rescue of DNA damage. This suggests a different mechanism for telomerase-mediated repair of *Eco*RI-induced damage as opposed to MMS, bleomycin, or HU-induced damage. One possibility for these results is the following: *Eco*RI generates perfectly complementary sticky ends with 4-base overhangs that can reanneal, creating a DNA segment containing two nicks, which can simply be ligated by the major ligase of yeast, Cdc9, independent of recombination or non-homologous end-joining (Figure 15). Overexpression of telomerase components could perhaps titrate an end-binding factor such as the Ku complex away from the DSB, similar to the previously mentioned damage-induced recombination-dependent model. However, if Est2 or Ten1 was titrating Ku, they would likely also repair damage-induced DSBs as in the *TLC1* recombination-dependent model. Titration of another end-binding protein such as Cdc13 is also a possibility, as Est2 can bind *TLC1,* and *TLC1* RNA interacts indirectly with Cdc13 through an interaction with Est1, and Ten1 interacts directly with Cdc13 (27). Future experiments in this area will attempt to determine the mechanism by which *TLC1*, Est2, and Ten1 rescue *Eco*RI-induced killing and whether other telomerase subunits, such as Est1 and Est3, can also influence DNA repair.

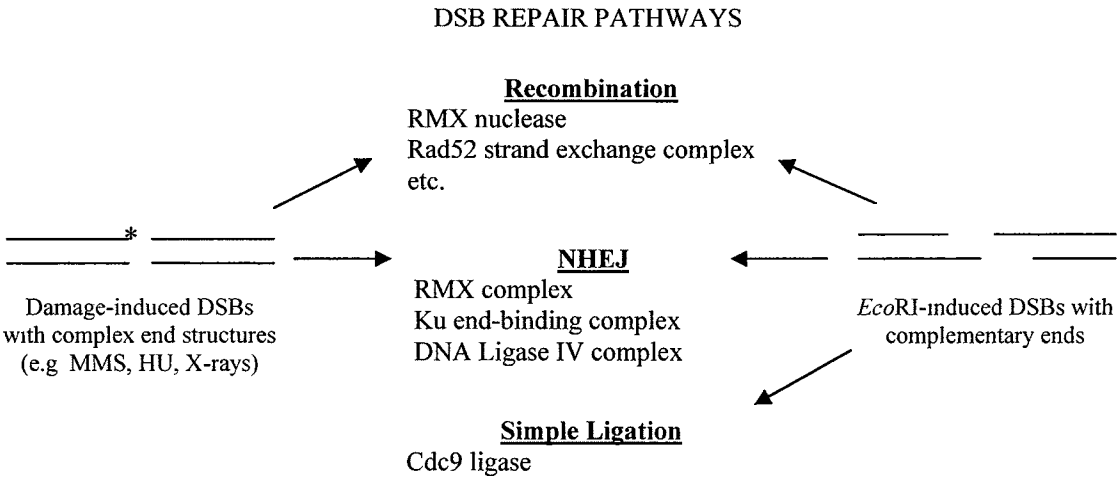

Figure 15. Pathways for repair of DSBs with damaged end structures (*) or with complementary overhangs. Recombination and NHEJ are utilized for damage produced by physical and chemical DNA-damaging agents. Restriction endonucleases producing complementary ends may be repaired by a simple ligation mechanism as well as recombination and NHEJ.

Catalytically inactive Est2 polymerase mutants are able to rescue the telomere instability of yku70 mutants grown at high temperature

Deletion of either of the Ku subunit genes, *YKU70* or *YKU80*, results in inactivation of the Ku complex. These mutants exhibit several phenotypes, including loss of transcriptional silencing at the ends of chromosomes, shortened telomeres, reduced NHEJ repair of DSBs, and high temperature sensitivity (12, 75). Ku is a known DNA end-binding protein that can associate with DSB ends and with telomeres *in vivo*, and is also involved in tethering of chromosome ends to the nuclear envelope (3, 76). Recent

evidence supports the idea that the temperature sensitivity phenotype (death at 37-40°C), involving arrest of growth in G_2 phase, is due to telomere stability defects rather than diminished ability to repair DNA damage due to decreased levels of NHEJ (77). Interestingly, overexpression of either *TLC1* RNA or Est2 has been shown to rescue Ku$^-$ temperature sensitivity (12, 43, 63). This could support the idea that Ku mutant telomeres become uncapped at this high temperature and overexpression of telomerase proteins is able to restore the telomeres to a capped state. Since the Ku complex is absent in these cells, the mechanism of telomerase rescue likely does not involve the stem-loop region of *TLC1* RNA as required for MMS or HU-induced damage rescue. The high temperature resistance could be in part due to telomerase-mediated extension of the shortened Ku telomeres, i.e., if more telomerase enzyme is synthesized, then short telomeres may be made longer and therefore stabilized. To provide more insight into this idea and to test other telomere-associated proteins as candidates for rescue of Ku$^-$ temperature sensitivity, pRS314 and overexpression plasmids for *TLC1* RNA (pLKL83Y), Est2 (pVL715), Ten1 (YEP195-Ten1), Stn1 (YEP195-Stn1), and Cdc13 (pVL459) were transformed into YLKL652 (Δ*yku70*) mutants. Cells were pronged onto synthetic plates at 30°C (normal growth temperature) and at 38°C. Cells were also grown in synthetic liquid media and analyzed using phase contrast microscopy to determine the percentage of cells in the G_2/M phase of the cell cycle when grown after 42 hours at 38°C.

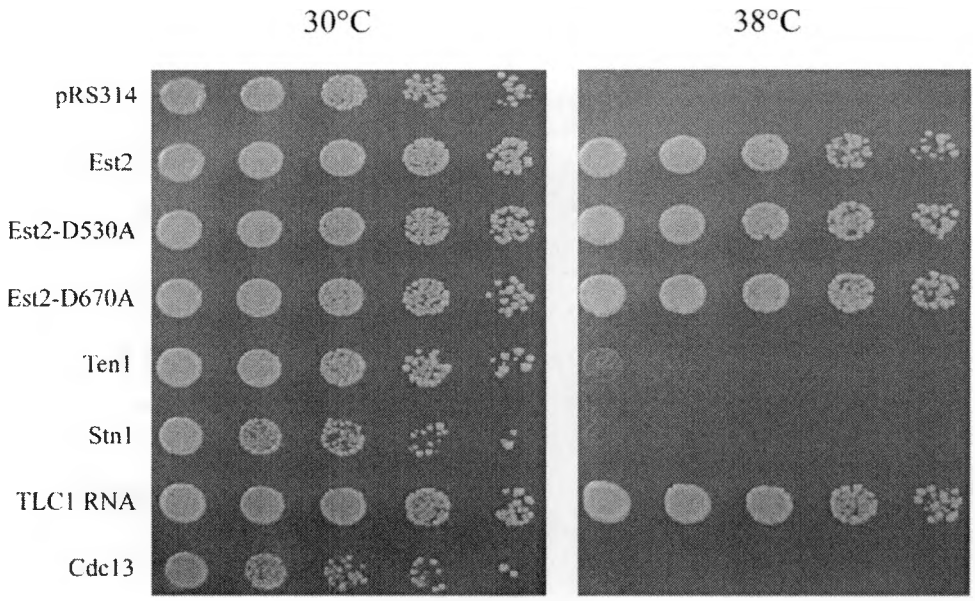

Figure 16. Effect of overexpression of Est2, inactive Est2 polymerase mutants, *TLC1* RNA, Stn1, or Ten1 on the temperature sensitivity phenotype of *yku70* cells. Overexpression of Est2, inactive Est2 polymerase mutants, or *TLC1* RNA alleviates the temperature sensitivity phenotype of *yku70* cells. Cdc13, Ten1, and Stn1 do not rescue *yku70* cells at 38°C.

As seen in Figure 16, *yku70* mutants containing the control vector pRS314 grew normally at 30°C, but died after transfer to 38°C. Overexpression of *TLC1* RNA or Est2 polymerase rescued *yku70* cells' temperature sensitivity, but Ten1, Stn1, and Cdc13 were ineffective.

As mentioned earlier, at elevated temperature, the DNA of *yku70* mutants becomes unstable. Changes in this structure are interpreted by the cells as damaged DNA and the cells undergo a DNA damage-induced cell cycle checkpoint arrest (63). The *yku70* cells eventually stop growing with most cells arresting in the G_2 phase of the cell cycle. The impact of overexpression of *TLC1*, Est2, Ten1, Stn1, and Cdc13 on cell cycle

arrest was investigated. As shown in Figure 17, high intercellular levels of Est2 or *TLC1* reduced the percentage of cells arrested in G2 after 42 hours at 38°C. In contrast, high level expression of Ten1, Stn1, or Cdc13 was unable to prevent G_2 arrest.

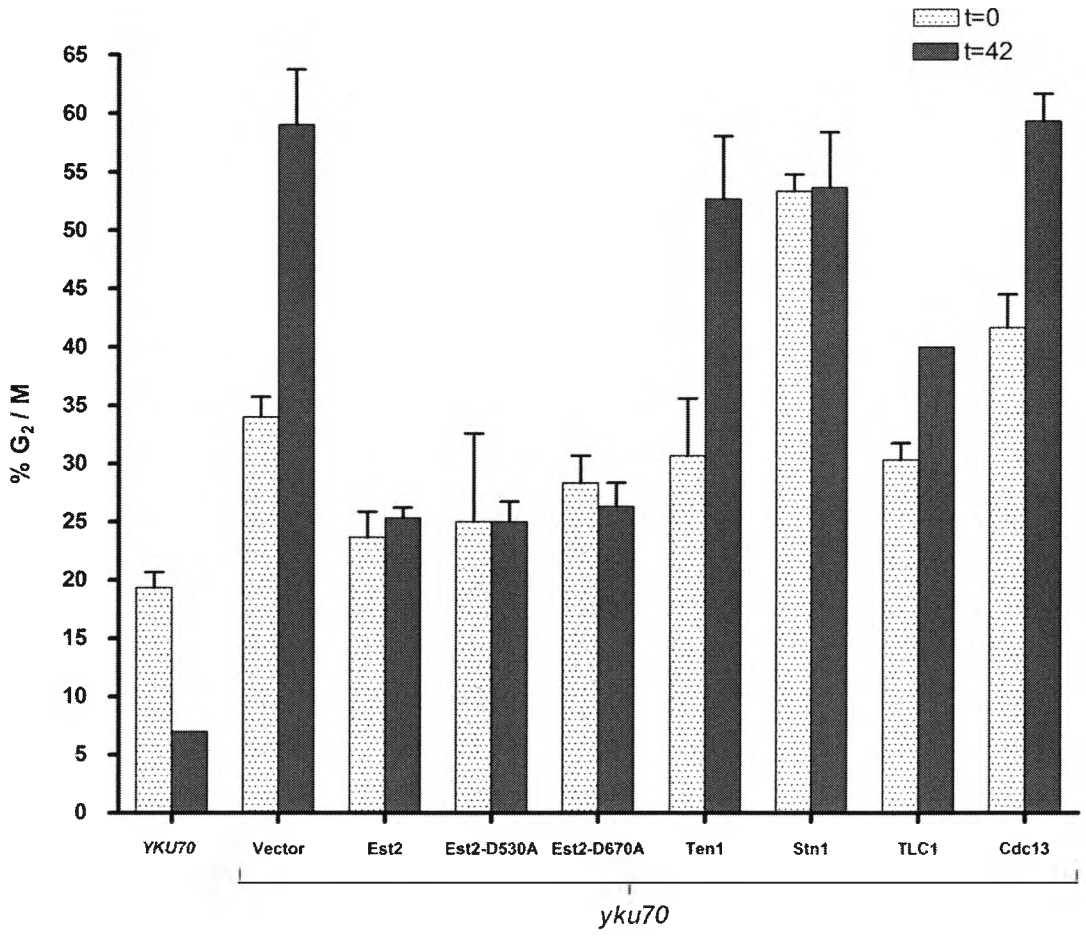

Figure 17. Effect of overexpression of Est2, inactive Est2 polymerase mutants, *TLC1* RNA, Stn1, or Ten1 on cell cycle arrest in *yku70* cells at 38°C. Percent of cells in G_2/M after exposure to 38°C. Cells were analyzed at t = 0 and 42 hr. Overexpression of Est2, inactive Est2 polymerase mutants, or *TLC1* RNA alleviates the temperature-induced G_2/M cell cycle arrest of *yku70* cells. Cdc13, Ten1, and Stn1 do not rescue G_2 arrest of *yku70* cells at 38°C.

The laboratory of Thomas Cech has identified and characterized several *est2* gene mutants that produce stable proteins *in vivo*, but the mutant proteins lack detectable polymerase activity (52). Two such mutants, Est2-D530A and Est2-D670A, have alterations in glutamic acid residues that are highly conserved among reverse transcriptase-like enzymes and these mutant proteins are catalytically inactive. It is possible that Est2 polymerase rescues the telomere instability of *ku* mutants by simply extending the ends of chromosomes to make them longer. Conceivably this could allow them to remain capped and/or tethered to the nuclear membrane at high temperatures. To test this possibility, overexpression plasmids pVL735 (Est2-D530A) and pVL743 (Est2-D670A) were transformed into *yku70* cells. As shown in Figure 9X (rows 3 and 4), each of the polymerase-deficient mutants was still able to rescue lethality at 38°C. Furthermore, they also eliminated the G_2 arrest response at elevated temperatures (Figure 17).

The rescue of *yku70* cells by enzymatically inactive Est2 polymerase mutants suggests that telomerase activity is not required. Thus the extension of Ku mutant's shortened telomeres by telomerase is not involved in the mechanism. Ku mutants are known to activate a Rad53p-dependent DNA damage checkpoint at high temperature, and this is suppressed by overexpression of *EST2* or *TLC1* (63; Figure 17). This along with the polymerase-defective Est2 data could support the previously mentioned model, where telomerase component overexpression restores the shortened Ku telomeres to a capped state at these high temperatures, presumably promoted by protein-protein interactions that have not yet been identified. This would keep the telomeres from becoming uncapped, thus not potentially appearing to the cell as a DSB and causing activation of DNA

damage responses. For further support, one might expect that overexpressing telomerase components in Ku^- cells could perhaps restore telomeric silencing, which is normally abolished in Ku mutants; however such was not the case (63).

Summary and Conclusions

Increased cellular levels of telomerase RNA had previously been shown to: reduce transcriptional silencing near telomeres, rescue loss of viability of *yku70/80* mutants at elevated temperatures, and increase cellular resistance to treatments that cause DSBs in *rad50*, *mre11*, or *xrs2* mutants. RMX mutants are extremely sensitive to agents that cause DSBs and also are known to have telomeres that are shorter than normal, indicating a role for RMX in normal telomere length maintenance.

Southern blot analysis revealed that overexpressing the telomerase components *TLC1* RNA or Est2 polymerase had no effect on telomere length in RMX mutants. Further analysis determined that *TLC1*-stimulated repair of DSBs produced by *Eco*RI versus MMS or HU may require different mechanisms.

MMS and HU-induced DNA damage required the recombination pathway for *TLC1* RNA-mediated repair. Analysis of *TLC1* RNA deletion derivatives suggested that the stem region was essential for the repair of MMS and HU-induced damage. Demonstration of the stem region's ability to rescue provided a further confirmation of the stem region's involvement, and the lack of rescue by the stem loop mutant imparted strong support for the requirement of an interaction with the Ku complex. Making use of the evidence at hand, our laboratory constructed a model of *TLC1* RNA-mediated repair of MMS and HU-induced damage in RMX cells (Figure 18).

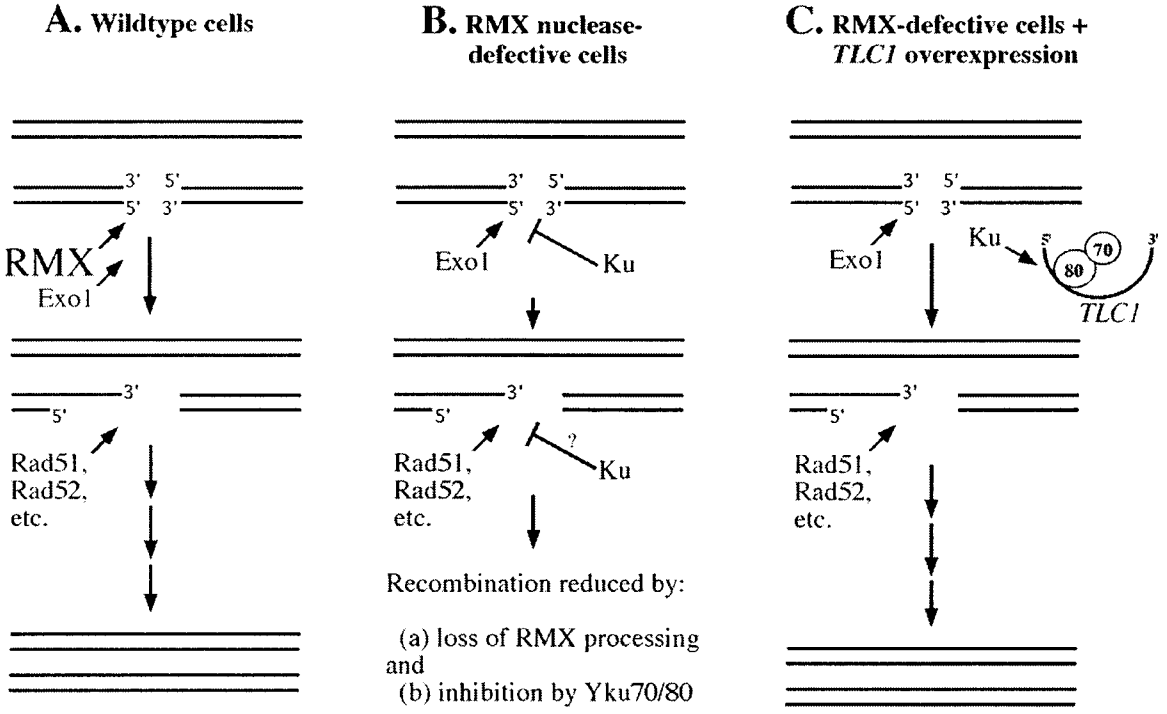

Figure 18. Models for repair of DSBs by homologous recombination.

(A) wildtype cells, (B) RMX-deficient mutants, and (C) RMX-deficient mutants overexpressing *TLC1* RNA.

As seen in Figure 18A, in wildtype cells, DSBs are first primarily acted upon by the nuclease activity of the RMX complex or to a lesser extent by the backup nuclease activity of Exo1. The resulting 3' overhangs provide substrates for the cellular recombination machinery to complete the repair process. In RMX-deficient cells (Figure 18B), Exo1 provides the nuclease activity required for recombinational repair in the absence of RMX, though it is much less efficient.

Historically, RMX mutants' sensitivity to X-rays, MMS, etc. was presumed to be due simply to the lack of DSB end-processing by Mre11. According to this new model,

this sensitivity is caused by two separate functions: loss of Mre11 processing and also inhibition of Exo1 processing by Ku. As the Ku complex is known to bind to DSBs, it may inhibit access of Exo1 and the recombinational machinery to the DSB. When *TLC1* RNA is overexpressed in RMX-deficient cells (Figure 18C), the molecules are capable of titrating the Ku complex away from the DSBs via interactions with their stem regions. This allows for better access of Exo1 and perhaps the recombinational proteins.

In conclusion, this study has provided insight into understanding the RMX complex and its interactions with telomerase in DSB repair. These results help to shed some light onto the complicated fields of research involving both telomerase and DNA repair, both of which aim to further our fundamental understanding of nature, and in turn could eventually aid in the treatment of human disorders characterized by defects in DNA repair.

REFERENCES:

1. Rassool, F.V. *Cancer Lett.* **2002**, 193, 1-9.

2. Lewis, L.K.; Resnick M.A. *Mutat Res.* **2000**, 451, 71-89.

3. Slijepcevic, P.; Bryant, P.E. *Int. J. Radiat. Biol.* **1998**, 73, 1-13.

4. Khanna, K.K.; Jackson, S.P. *Nat. Genet.* **2001**, 27, 247-254.

5. Botstein, D.; Chervitz, S.A.; Cherry, J.M. *Science* **1997**, 277, 1259-1260.

6. Hopfner, K.P.; Craig, L.; Moncalian G.; Zinkel, R.A.; Usui, T.; Owen, B.A.; Karcher, A.; Henderson, B.; Bodmer, J.L.; McMurray, C.T.; Carney, J.P.; Petrini, J.H.; Tainer, J.A. *Nature* **2002**, 418, 562-566.

7. Furuse, M.; Nagase, Y.; Tsubouchi, H.; Murakami-Murofushi, K.; Shibata, T.; Ohta, K. *EMBO J.* **1998**, 17, 6412-6425.

8. Lobachev, K.S.; Gordenin D.A.; Resnick M.A. *Cell* **2002**, 108, 183-193.

9. Diede, S.J.; Gottschling, D.E. *Curr. Biol.* **2001**, 11, 1336-1340.

10. Tsukamoto, Y.; Mitsuoka, C.; Terasawa, M.; Ogawa, H.; Ogawa, T. *Mol. Biol. Cell* **2005**, 16, 597-608.

11. Chen C.; Trujillo, K.; Ramos, W.; Sung, P.; Tomkinson, A.E. *Mol. Cell* **2001**, 8, 1105-1115.

12. Lewis, L.K.; Karthikeyan, G.; Westmoreland, J.W.; Resnick, M.A. *Genetics* **2002**, 160, 49-62.

13. Lewis, L.K.; Storici, F.; Van Komen, S; Calero, S.; Sung, P.; Resnick, M.A. *Genetics* **2003**, 166, 1701-1713.

14. Symington, L.S. *Microbiol. Mol. Biol Rev.* **2002**, 66, 630-670.

15. Le S.; Moore, J.K.; Haber, J.E.; Greider, C.W. *Genetics* **1999**, 152, 143-152.

16. Taylor, A.M. *Best Pract. Res. Clin Haematol.* **2001,** 14, 631-644.

17. Griffith, J.D.; Comeau, L.; Rosenfield, S.; Stansel, R.M.; Bianchi, A.; Moss, H.; de Lange, T. *Cell* **1999**, 97, 503-514.

18. Blackburn, E.H. *Nature* **2000**, 408, 53-56.

19. Cawthon, R.M.; Smith, K.R.; O'Brien, E.; Sivatchenko, A.; Kerber, R.A. *Lancet* **2003**, 361, 393-395.

20. Sandell, L.L.; Zakian, V.A. *Cell* **1993**, 75, 729-739.

21. Guilleret, I.; Benhattar, J. *Exp. Cell Res.* **2003**, 289, 326-334.

22. Asai, A.; Oshima, Y.; Yamamoto, Y.; Uochi, T.; Kusaka, H.; Akinaga, S.; Yamashita, Y.; Pongracz, K.; Pruzan, R.; Wunder, E.; Piatyszek, M.; Li, S.; Chin, A.C.; Harley, C.B.; Gryaznov, S. *Cancer Res.* **2003**, 63, 3931-3939.

23. Shea, B.; Herbert; Gellert, G.C.; Hochreiter, A.; Pongracz, K.; Wright, W.E.; Zielinska, D.; Chin, A.C.; Harley, C.B.; Shay, J.W.; Gryaznov, S.M. *Oncogene* **2005**, 24, 5262-5268.2

24. Geron Corporation. *Safety and Dose Study of GRN163L Administered Weekly to Treat Patients With Chronic Lymphocytic Leukemia (CLL).* In: ClinicalTrials.gov [Internet]. Bethesda (MD): National Library of Medicine; **2000**- [cited 2006 June 30]. Available from: http://clinicaltrials.gov/show/NCT00124189 NLM Identifier: NCT00124189.

25. Geron Corporation. *Safety and Dose Study of GRN163L Administered Weekly to Treat Patients With Solid Tumor Malignancies* In: ClinicalTrials.gov [Internet]. Bethesda (MD): National Library of Medicine; **2000**- [cited 2006 June 30]. Available from: http://clinicaltrials.gov/show/ NCT00310895 NLM Identifier: NCT00310895.

26. P. Dahm. *Active Immunotherapy with Human LAMP Telomerase RNA-Transfected Immature, Autologous Dendritic Cells Primed in situ Using Escalating Doses of the Topical Immunostimulant Imiquimod (Aldara™) in Patients with Prostate Cancer.* In: Dukecancervaccines.org [Internet]. Raleigh (NC): Duke University; [cited **2006** June 30]. Available from: http://www.dukecancervaccines.org/trial_prostate.htm

27. Grandin, N.; Damon, C.; Charbonneau, M. *EMBO J.* **2001**, 201, 173-183.

28. Cech, T. R. *Cell* **2004**, 116, 273-279.

29. Prescott, J.; Blackburn, E.H. *Genes & Dev.* **1997**, 11, 528-540.

30. Chappell A.S.; Lundblad, V. *Mol. Cell Biol.* **2004**, 24, 7720-7736.

31. Zhou, J.; Hidaka, H.; Futcher, B. *Mol. Cell Biol.* **2000**, 20, 1947-1955.

32. Vitra-Pearlman, V.; Morris, D.K.; Lundblad, V. *Genes & Dev.* **1996**, 10, 3094-3104.

33. Singh, S.M.; Lue, N.F. *PNAS* **2003**, 100, 5718-5723.

34. Evans S.K.; Lundblad, V. *Science* **1999**, 286, 117-20.

35. Pennok E.; Buckley, K.; Lundblad, V. *Cell* **2001**, 104, 387-396.

36. Yang, C.; Chen, Y.; Meng, F.; Zhou, F. *NAS* **2006**, 34, 407-416.

37. Friedman, K.L.; Heit, J.J.; Long, D.M.; Cech, T.R. *Mol. Biol. Cell* **2003**, 14, 1-13.

38. Hopfner, K.; Putnam, C.D.; Tainer, J.A. *Curr. Opin. Struct. Biol.* **2002**, 12, 115-122.

39. Peterson, S.E.; Stellwagen, A.E.; Diede, S.J.; Singer, M.S.; Haimberger, Z.W.; Johnson, C.O.; Tzoneva, M.; Gottschling, D.E. *Nat. Genet.* **2001**, 27, 64-67.

40. Bertuch, A.A.; Lundblad, V. *Genetics* **2003**, 166, 1651-1659.

41. Kazunori, T.; Matsuura, A.; Caspari, T.; Carr, A.M.; Akamatsu, Y.; Iwasaki, H.; Mizuno, K.; Ohta, K.; Uritani, M.; Ushimaru, T.; Yoshinaga, K.; Ueno, M. *Mol. Cell Biol.* **2003**, 23, 5186-8197.

42. Singer M.S.; Gottschling, D.E. *Science* **1994**, 266, 404-409.

43. Nugent C.I.; Bosco G.; Ross L.O.; Evans S.K.; Salinger A.P.; Moore J.K.; Haber J.E.; Lundblad V. *Curr. Biol.* **1998**, 8, 657-660.

44. Cassiano, J. M.S. thesis, Texas State University, San Marcos, TX, **2004**.

45. Brachmann C.B.; Davies A.; Cost G.J.; Caputo E.: Li J.; Hieter P.; Boeke, J.D. *Yeast* **1998**, 30, 115-132.

46. Larionov V.; Kouprina N.; Nikolaishvili N.; Resnick, M.A. *Nucleic Acids Res.* **1994**, 22, 4154-4162.

47. Schiestl, R.H.; Reynolds, P.; Prakash, S.; Prakash, L.; *Mol. Cell. Biol.* **1989**, 9, 1882-1896.

48. Morrison, A.; Sugino, A. *Mol. Gen. Genet.* **1994**, 242, 289-296.

49. Sikorski R.S.; Hieter, P. *Genetics* **1989**, 122, 19-27.

50. Christianson, T.W.; Sikorski, R.S.; Dante, M.; Shero, J.H.; Hieter, P. *Gene* **1992**, 110, 119-122.

51. Chandra, A.; Hughes, T.R.; Nugent, C.I.; Lundblad, V. *Genes & Dev.* **2001**, 15, 404-414.

52. Lingner, J.; Hughes, T.R.; Shevchenko, A.; Mann, M.; Lundblad, V.; Cech, T.R. *Science* **1997**, 276, 561-567.

53. Tishkoff D.X.; Boerger A.L.; Bertrand P.; Filosi N.; Gaida G.M.; Kane M.F.; Kolodner R.D. *Proc. Natl. Acad. Sci.* **1997**, 94, 7487-7492.

54. Grandin, N.; Damon, C.; Charbonneau, M. *EMBO J* **2001**, 20, 6127-6139.

55. Singer M.S.; Kahana, A.; Wolf, A.J.; Meisinger, L.L.; Peterson, S.E.; Goggin, C.; Mahowald, M.; Gottschling, D.E. *Genetics* **1998**, 150, 613-632.

56. Sambrook, J.; Russell, D.W. *Molecular Cloning: A Laboratory Manual*; 3rd ed; Cold Spring Harbor Laboratory Press: Cold Spring Harbor; NY, **2001**.

57. Gietz, R.D.; Schiestl, R.H.; Willems, A.R.; Woods, R.A. *Yeast.* **1995,** 11, 355-360.

58. Soni, R.; Carmichael, J.P.; Murray, J.A. *Curr Genet.* **1993,** 24, 455-459.

59. Chung, C.T.; Niemela, S.L.; Miller, R.H. *Proc. Natl. Acad. Sci.* **1989**, 86, 2172-2175.

60. Goldstein A.L.; McCusker, J.H. *Yeast* **1999**, 15, 1541-1553.

61. Alani, E.; Cao, L.; Kleckner, N. *Genetics* **1987**, 116, 541–545.

62. Wach A.; Brachat, A.; Pohlmann, R.; Philippsen, P. *Yeast* **1994**, 10, 1793-1808.

63. Teo, S.H.; Jackson, S.P. *EMBO Rep.* **2000**, 2, 197-202.

64. Boeke J.D.; Trueheart J.; Natsoulis G.; Fink G.R. *Methods Enzymol.* **1987**, 154, 164-175.

65. Boulton, S.J.; Jackson, S.P. *EMBO J.* **1998**, 6, 1819-1828.

66. Beranek, D.T. *Mutat. Res.* **1990**, 231, 11-30.

67. Pascucci, P.; Russo, M.T.; Crescenzi, M.; Bignami, M.; Dogliotti E. *Nucleic Acids Res.* **2005**, 33, 280-288.

68. Lundin C.; Erixon K.; Arnaudeau C.; Schultz N.; Jenssen D.; Meuth M.; Helleday T. *Mol. Cell Biol.* **2002**, 16, 5869-5878.

69. Giloni L.; Takeshita M.; Johnson F.; Iden C.; Grollman A. P. *J. Biol. Chem.* **1981**, 256, 8608-8615.

70. Burger R. M. *Chem. Rev.* **1998**, 98, 1153-1169.

71. Nicholas S. Y.; Yu, Y.; Pohorelic, B.; Lees-Miller, S.P.; Beattie, T.L. *Nucleic Acids Res.* **2005**, 33, 2090-2098.

72. Stellwagen, A.E.; Haimberger, Z.W.; Veatch, J.R.; Gottschling, D.E. *Genes & Dev.* **2003**, 17, 2384-2395.

73. Maringele, L.; Lydall, D. *Gene Dev.* **2002**, 16,1919-1933.

74. Calero, S. M.S. thesis, Texas State University, San Marcos, TX, **2003**.

75. Fellerhoff, B.; Eckardt-Schupp, F.; Friedl, A.A. *Genetics* **2000**, 154, 1039-1051.

76. Galy V.; Olivo-Marin J.C.; Scherthan H.; Doye V.; Rascalou N.; Nehrbass U. *Nature* **2000**, 403, 108-112.

77. Gravel, S.; Wellinger, R.J. *Mol. Cell Biol.* **2002**, 22, 2182-2193.

VITA

Brian Michael Wasko was born in Houston, Texas on May 29, 1981. He is the son of Mary Elizabeth Wasko and William Joseph Wasko. He graduated from Dickinson High School in Dickinson, Texas in 1999. In 2004, he graduated from Texas State University-San Marcos with a Bachelor of Science degree with a major in biochemistry and minor in business administration. During the fall of 2004 he entered graduate school at Texas State University-San Marcos in the Department of Chemistry and Biochemistry.

Permanent Address: 5414 Thistle Dr.
Dickinson, TX 77539

This thesis was typed by Brian Michael Wasko.